

**Thermal Performance and Pressure Drop of the Compact Heat Exchangers based on
DMLS**

by

Kailai Yang

Bachelor of Engineering, Huazhong University of Science and Technology, 2018

Submitted to the Graduate Faculty of the
Swanson School of Engineering in partial fulfillment
of the requirements for the degree of
Master of Science in Mechanical Engineering

University of Pittsburgh

2020

UNIVERSITY OF PITTSBURGH

SWANSON SCHOOL OF ENGINEERING

This thesis was presented

by

Kailai Yang

It was defended on

April 3, 2020

and approved by

Minking Chyu, PhD, Professor,

Department of Mechanical Engineering and Materials Science

Qing-Ming Wang, PhD, Professor

Department of Mechanical Engineering and Materials Science

Patrick Smolinski, PhD, Associate Professor

Department of Mechanical Engineering and Materials Science

Thesis Advisor: Minking Chyu, PhD, Professor

Department of Mechanical Engineering and Materials Science

Copyright © by Kailai Yang

2020

Thermal Performance and Pressure Drop of the Compact Heat Exchangers based on DMLS

Kailai Yang, MS

University of Pittsburgh, 2020

In recent years, direct metal laser sintering (DMLS) has been gradually applied to various fields as an advanced additive manufacturing method. In this study, four printed-circuit-heat-exchanger like (PCHE-like) compact heat exchangers with different channel structures were designed and manufactured by the DMLS method. Performance tests were carried out to compare the thermal performance and pressure drop of these four compact heat exchangers. The compact heat exchangers were tested for air flow rate in the range of 6.5 to 37.7 L/min keeping the hot-side and cold-side inlet temperature fixed at 52 °C and 25 °C, respectively. It was found that the heat exchanger with the most densely arranged circular straight channels had better heat transfer performance and lower pressure drop. Later, scanning electronic microscope (SEM) images and image segmentation techniques were employed to evaluate the surface roughness and geometric features of the heat exchanger channels manufactured by the DMLS method. It showed that the build direction had a great impact on the final quality of the manufactured channel. Channels built in the vertical direction had less surface roughness and geometric feature changes compared to the channels built in the horizontal direction. In addition, comparative study demonstrated that the surface roughness and geometric feature changes of the circular channels were larger than those of the semicircular channels when they were built in the same direction and had the same design hydraulic diameter of 1mm. Finally, circular and semicircular channels with different DMLS built direction were tested to determine their flow resistance by using the Fanning friction factor.

Vertically built circular channels showed minimal resistance, while horizontally built circular channels showed maximum resistance.

Table of Contents

Acknowledgments	viii
Nomenclature	ix
1.0 Introduction.....	1
1.1 Project Background	1
1.2 Literature Review.....	4
2.0 Theoretical Analysis and Geometric Design	9
2.1 Theoretical Analysis.....	9
2.1.1 Convection Heat Transfer Theory Analysis	9
2.1.2 Theoretical Calculation Formula	13
2.2 Compact Heat Exchangers Design.....	17
2.2.1 Flow Arrangement	17
2.2.2 Channel Cross-sectional Shape.....	20
2.2.3 Wall Thickness between Channels	23
3.0 Research Description.....	25
3.1 Objective.....	25
3.2 Tasks	25
4.0 Experimental Details	27
4.1 Compact Heat Exchangers Manufactured by DMLS Method	27
4.1.1 Four Types of Compact Heat Exchanger Designs	28
4.1.2 Experiment Setup and Conditions.....	31
4.1.3 Experiment Results and Discussion.....	34

4.2 Surface Roughness and Geometric Feature of Channels	41
4.2.1 Surface Roughness and Geometric Feature Evaluation.....	44
4.2.2 Pressure Drop Characteristics	51
5.0 Conclusion	55
Bibliography	57

List of Tables

Table 1 Comparison of laminar-flow solutions for different cross-sectional shape	21
Table 2 Design parameter table of compact heat exchanger	30

List of Figures

Figure 1 Typical temperature distributions in heat exchangers	19
Figure 2 Photograph of the compact heat exchangers	27
Figure 3 Four different types of compact heat exchangers investigated in this study	29
Figure 4 Total number of channels and total heat transfer area of compact heat exchanger	31
Figure 5 Model of the experimental setup test section	33
Figure 6 Photograph of the experimental setup.....	33
Figure 7 Schematic diagram of the experimental setup	34
Figure 8 Temperature chart	34
Figure 9 Heat exchanger effectiveness and the overall heat transfer coefficient with the same flow rate	35
Figure 10 Average heat transfer rate and the overall heat exchanger conductance with the same Reynolds number.....	36
Figure 11 Average pressure drop with the same flow rate on hot and cold sides.....	37
Figure 12 Average Fanning friction factor with the same Reynolds number on hot and cold sides	38
Figure 13 Relative performance coefficient η with the same flow rate.....	39
Figure 14 Cross-sectional view of the heat exchangers investigated in this study	41
Figure 15 Inner view of the channel through microscope.....	42
Figure 16 Morphology differences between channels with different build directions and geometric shapes	43

Figure 17 Illustrative graph for heat exchangers cutting.....	45
Figure 18 Designed profiles for different channels	46
Figure 19 Examples of actual profiles for circular channel.....	47
Figure 20 Examples of actual profiles for semicircular channel	48
Figure 21 Comparison of hydraulic radius for different channels.....	50
Figure 22 Comparison of surface roughness for different channels	50
Figure 23 Comparison of pressure drops with the same Reynolds number	52
Figure 24 Comparison of the Fanning friction factors with the same Reynolds number	53

Acknowledgments

I would have great and sincere thanks to my advisor, Dr. Minking Chyu for his patience, generousness and invaluable guidance throughout my study and research. Our conversation has always been friendly and meaningful, and it will benefit my life.

I would also thank my committee members Dr. Qing-Ming Wang and Dr. Patrick Smolinski for their time to make this thesis better.

I am also extremely grateful to my excellent upper class students in my research group: Zheng Min, Sarwesh Parbat. Without their help and encouragement in this research, I would have never accomplished my research.

Finally, I would like to thank my family and my girlfriend for their unconditional support and love.

Nomenclature

A	Heat transfer area
A_{ch}	Cross-sectional area of flow channel
A_f	Free flow area
C	Fluid heat transfer capacity rates
C_p	Specific heat
C_r	Heat capacity-rate ratio
D_h	Hydraulic diameter
E	Joint efficiency
f	Fanning friction factor
f_D	Darcy or Moody's friction factor
h	Convective heat transfer coefficient
k	Thermal conductivity of the fluid
k_s	Thermal conductivity
L	Actual length of the channel
\dot{m}	Mass flow rate
N_{ch}	Number of channels on one side
Nu	Nusselt number
NTU	Number of transfer units
P	Internal design pressure
P_{ch}	Cross-sectional perimeter of the flow channel

Δp	Pressure drop
Q	Heat exchange rate
Q_{loss}	Heat loss
Q_m	Average heat exchange rate
R	Channel radius
Ra	Arithmetical deviation of profile
R_h	Hydraulic radius
R_m	Mean radius
Re	Reynolds number
S	Maximum allowable stress
T	Fluid temperature
ΔT_m	Logarithmic mean temperature difference
t	Solid wall thickness
U	Overall heat transfer coefficient
UA	Overall heat exchanger conductance
V	Heat exchanger volume
v	Fluid velocity
β	Heat transfer surface area density
ε	Heat exchanger effectiveness
ρ	Fluid density
μ	Dynamic viscosity
Subscripts	
c	Cold fluid

<i>h</i>	Hot fluid
<i>in</i>	Inlet
<i>out</i>	Outlet
<i>max</i>	maximum
<i>min</i>	Minimum
<i>circle</i>	Circular channel
<i>semicircle</i>	Semicircular channel

1.0 Introduction

1.1 Project Background

Heat exchanger is a device used to transfer the heat of high temperature fluid to low temperature fluid. It is a heat transfer device widely used in power systems, chemical processing, manufacturing industries and other industrial sectors, or as air conditioners, refrigerators and radiators indispensable in modern life. Although the shell-and-tube type heat exchanger is the most widely used heat exchanger, due to its large volume, it is inferior to some plate heat exchangers and new high-efficiency heat exchangers in terms of compact structure, heat exchanger effectiveness and metal consumption per unit heat transfer area. Therefore, shell-and-tube heat exchangers have gradually been replaced by other more efficient and compact heat exchangers. A compact heat exchanger with a large ratio of heat transfer surface area per unit volume can reduce the installation space, weight, energy requirements and costs, thus improving plant layout and processing conditions and operating efficiency. For the definition of compact heat exchangers, several researchers have proposed different standards for compact heat exchangers. D. A. Reay et al. [1] proposed that compact heat exchangers are defined as the units with a surface area density larger than $700 \text{ m}^2/\text{m}^3$ when operating in gas streams, or larger than $300 \text{ m}^2/\text{m}^3$ when operating in the liquid or two-phase streams. However, some heat exchangers with a surface area density larger than $200 \text{ m}^2/\text{m}^3$ can also be considered as compact heat exchangers. Mehendale et al. [2] classified the heat exchangers with hydraulic diameters from 1mm to 6mm as compact heat exchangers. In summary, the compact heat exchanger is a general term for the heat exchanger with a large ratio of heat transfer surface area to volume.

Printed Circuit Heat Exchanger (PCHE) is one type of compact heat exchanger, which is classified as a plate heat exchanger, developed as a replacement for shell-and-tube heat exchangers. Because the compactness of this heat exchanger ranges from 200 to 5000 m²/m³ according to different structural designs[3], which is usually larger than traditional shell-and-tube heat exchangers[1], meeting the expectations of high efficiency and compactness. The manufacturing method of PCHE is mainly to etch out the fluid channels on one side of each plate by chemical etching, and then stack the etched plates in the required order. Finally, by employing the diffusion bonding method, the contact surfaces between adjacent plates are fused with each other to form a strong and compact heat exchanger core. The flow channel characteristics of PCHE are the main factors affecting the heat transfer and flow resistance characteristics of heat exchangers. The layout of the flow channel mainly can be designed as parallel-flow, counter-flow and cross-flow. Among them, cross-flow is the most common flow arrangement, because it greatly simplifies the design of the header at the inlet and outlet of each fluid[3]. Currently, the types of PCHE channels include the straight, zigzag, wavy or airfoil. Among them, the straight shape is the simplest flow channel structure of PCHE. The structural parameters of the PCHE flow channel include cross-sectional shape, hydraulic diameter, and channel interval. The cross-section of the PCHE channel is usually a semicircular shape with a diameter of 0.5 to 2 mm. The longitudinal interval between the channels is limited by the thickness of the individually assembled plates, which is typically greater than 1.6 mm[3]. Therefore, in actual manufacturing or simulation research, many researchers have set the longitudinal interval to 1.6 mm or more [4–7]. The channel pitch is selected according to the performance requirements and operating conditions. At present, the heat exchanger effectiveness of PCHE can achieve higher than 97%, and the maximum working temperature and pressure can reach 1000 °C and 500 bars, respectively[8]. The main material for manufacturing

PCHE is 300 series austenitic stainless steel, such as SS304, SS316, SS316L. Various other feasible metals include 22 chromium duplex metals, copper nickel, nickel alloys, and titanium[9]. Because PCHE adopts diffusion bonding to stack the etched flat metal plates into the heat exchanger core, improving the stability of the weld seam, which makes it meet the requirements of safety and reliability under high-pressure conditions. Due to the high heat exchanger effectiveness provided by such advanced heat exchanger design under high pressure and limited space conditions, PCHE has been applied in the fields of liquefied natural gas industry, aerospace, chemical processing, nuclear power and solar power generation.

Photochemical machining (PCM) and diffusion bonding are the two main techniques used to fabricate PCHE. The PCM is a chemical milling process, normally performed in a series of eight steps: cutting, cleaning, coating, photo-tooling, exposing, developing, photo-etching and stripping[10]. Due to the effect of the strong chemical etchants, the average surface roughness of the channels etched on the metal plate is less than a micrometer[11]. However, the disadvantage of PCM is that the etchant will not only corrode the metal downwards, but also corrode sideways[12], which limits the design of the channel cross-sectional shape. More importantly, the strong chemical etchants are very dangerous to workers[13]. For diffusion bonding, this is a solid-state joining process where two flat surfaces are bonded with high pressure at an elevated temperature[14]. For example, Mylavarapu et al.[15] fabricated two heat exchangers by diffusion bonding. During the manufacturing process, the metal parts were heated to about 1120 °C and kept bonded for four hours under the pressure of 6.8 to 10.2 MPa. Considering the operation conditions of these two techniques, it is obvious that in addition to industrial production, the manufacture of PCHE is difficult and might be dangerous in an academic laboratory setting.

In recent years, direct metal laser sintering (DMLS), as one of the most promising metallic additive manufacturing technologies, has gradually been applied to various fields. This technology mainly uses laser beam to sinter metal powder into a solid part layer by layer, which can directly produce complex features according to CAD model, leading to a significant reduction in time[16-17]. Compared with traditional manufacturing technologies, DMLS has the advantages of simple production steps, high flexibility of product design and the possibility to manufacture metal parts with high dimensional accuracy and geometric complexity[18-19]. In addition, the entire manufacturing process is automatic, which greatly benefits the fabrication process[20]. Hence, DMLS has great application potential in many fields such as biomedical, automotive, energy, consumer goods and aerospace[21]. For compact heat exchangers manufacturing, using the DMLS method will not only simplify the fabrication steps but will also provide the possibility of designing complex channel structures. Moreover, DMLS method allows the heat exchanger to be manufactured directly as an integrated device, which can eliminate the difficulties for assembly. Therefore, it is worth considering utilizing the DMLS method instead of the traditional PCHE manufacturing method to construct compact heat exchangers with the similar structure.

1.2 Literature Review

Among the previous studies on compact heat exchangers, Reay et al. [1] summarized a number of compact heat exchangers with different types. Compared with traditional shell and tube heat exchangers, their area density is greater than $200 \text{ m}^2/\text{m}^3$, which greatly improved the efficiency and reduced the volume and weight of the heat exchanger. The particular PCHE cited in [1] played a significant role in reducing the cost of a heat pump system.

Yoon et al.[22] developed a cross-flow PCHE analysis code to evaluate the size and cost of the heat exchanger by utilizing MATLAB software. The information provided by this code can be used to optimize the design of advanced small modular reactors (SMRs) systems.

Tsuzuki et al.[6] carried out simulations using FLUENT CFD-based software to compare the PCHE with discontinuous S-shape flow channel configuration to the conventional continuous zigzag configuration. Their results suggested that the pressure drop in S-shape flow channels was one-fifth that in zigzag channels, while the thermal performance was about equal. The reverse flows and eddies occurring around bend corners of zigzag flow channels are the main causes for the increased pressure drop.

Wang et al.[23] conducted a numerical simulation to investigate the thermal-hydraulic performance of the sinusoidal channel PCHE. They found that the overall Nusselt number was enhanced by 7.4% to 13.9%, while the global Fanning friction factor increased by 10.9% to 16.7% compared to the straight channel PCHE. Their results suggested that under the condition of the same length, the heat transfer capacity improvement of sinusoidal channel compared to the straight channel was attributable to the higher level of local turbulence intensity around the curved corners.

Lee et al.[24] performed a comparative study on the performance of a zigzag PCHE with various channel cross-sectional shapes (semicircular, circular, rectangular and trapezoidal) using CFD simulation. They reported that the PCHE with a rectangular channel cross section had the highest effectiveness, while the PCHE with a circular channel cross section had the lowest effectiveness among the four different shapes. However, in terms of friction factors, the circular channel had the smallest friction factor, suggesting the flow resistance in the channel is the lowest.

Berbish et al.[25] performed an experimental study on forced convection heat transfer and pressure drop characteristics of airflow in a horizontal semicircular duct to obtain empirical

correlations for the heat transfer coefficient and friction factor as a function of the Reynolds number. By comparing with the empirical correlations for straight circular duct proposed by Reynolds[26] and Blasius[27], they found that both the Nusselt number and the friction factor of the semicircular tube were slightly higher, due mainly to the effects of the sharp edges of the semicircular duct that distorted the axial velocity profile.

Kim et al.[28] performed a numerical analysis using CFD simulation. They found that the numerical simulation of the traditional zigzag PCHE differed from the experimental data by about 10%. They also studied a PCHE model filled with airfoil-shaped flow channels in comparison with the typical zigzag flow channels. Their results suggested that for a given heat exchange rate per unit volume, the pressure drop in the airfoil-based PCHE was only one-twentieth of that in the traditional zigzag-channeled PCHE. The plausible reason is that the airfoil shape suppresses the separation of flow, which occurred at the corners of the zigzag channels, thereby reducing the pressure loss.

Seo et al.[29] conducted a study on heat transfer and pressure drop characteristics in straight channel of PCHE with different flow arrangements. They found that the heat transfer performance of the counter-flow PCHE was 10% to 15% higher than that of the parallel-flow PCHE.

Kim et al. [30] conducted a study on the thermal-hydraulic performance of the PCHE using a helium test facility. They proposed two empirical correlations for the average Fanning friction factor and average Nusselt number in laminar flow region. Each empirical correlation consisted of a constant term and a functional term. The constant term was related to the geometrical characteristics of the straight portion of the PCHE channel, such as the channel cross-sectional

shape. The functional term was related linearly to the Reynolds number due to the form loss at sharp elbows in the zigzag channel.

For the recent research on channels or heat exchangers manufactured through DMLS method, Utilizing CT scan, Snyder et al.[31] conducted a study on the influence of DMLS build direction on the heat transfer coefficient and pressure loss in small-scale channels. They indicated that the channels with vertically build direction had the lowest friction factor, while the channels with diagonally build direction had the highest friction factor. However, large differences in friction factors caused by build directions did not produce similar differences in Nusselt numbers. Somewhat unexpectedly, the heat transfer performance of these channels was almost the same.

Kirsch et al.[32] conducted a study on the heat transfer and pressure loss performance of wavy channels manufactured through DMLS. They found that the wavy channels improved heat transfer but also introduced higher pressure loss compared to the straight channels. Among them, short-wavelength channels introduced high pressure losses without noticeable improvement in heat transfer, while long-wavelength channels provided good heat transfer performance with a less penalty in pressure drop.

Stimpson et al.[33] carried out experiments for roughness effects on flow resistance and heat transfer in DMLS manufactured channels. They manufactured ten different coupons with rectangular channels, measured the surface roughness levels through CT scans, and then compared the friction factor and heat transfer performance of these coupons. Results indicated that compared with the smooth channels, the friction factors of these channels had been significantly increased, causing higher pressure losses. Although the roughness improved the heat transfer coefficient to some extent, the increase in heat transfer coefficient did not match with the increase in the friction factor, as it.

Zhang et al.[34] manufactured a compact gas-to-gas heat exchanger through DMLS and tested it at 600 °C with 450 kPa inlet pressure. The maximum heat duty and heat transfer density

of this heat exchanger are 2.78 kW and 10 kW/kg, respectively. This work demonstrated the possibility of using DMLS to fabricate compact heat exchangers

2.0 Theoretical Analysis and Geometric Design

2.1 Theoretical Analysis

2.1.1 Convection Heat Transfer Theory Analysis

For a compact heat exchanger like PCHE, it can be classified as a surface type heat transfer device. Inside a heat exchanger, the two fluids are separated by a solid wall. Its heat transfer principle is that the hot fluid first transfers heat to the wall surface through convective heat transfer. After conducting in the solid wall, the heat is then transferred to the cold fluid from another solid wall surface through convective heat transfer. Convective heat transfer can refer to the transfer of heat from a fluid to a solid wall, which is driven by the movement of the fluid. There are many factors affecting convection heat transfer, which can be summarized as follows [35]:

(1) Causes of fluid flow

According to different flow causes, convective heat transfer can be divided into natural convective heat transfer and forced convective heat transfer. Natural convection heat transfer is due to the uneven distribution of temperature or concentration in the flow field, which makes the fluid density distribution vary greatly. Consequently, the fluid will flow naturally and exchange heat with the solid wall under the influence of temperature difference. In forced convective heat transfer, the fluid is forced to flow over and exchange heat with the surface of solid wall by external means such as pumps, fans, suction devices or others. When the causes of fluid flow are different, the velocity and state distribution of the fluid will be different, which will lead to different heat transfer effects.

(2) Phase transition of fluid

In the process of heat exchange, if the fluid has no phase change, its heat exchange is realized through the change of the sensible heat of the fluid. In another case, if the fluid undergoes a phase change during the heat exchange process, such as evaporation or condensation, the change in the latent heat of the fluid at this time will have a greater impact on the heat exchange.

(3) Flow state of fluid

When the fluid is viscous, its flow state can be divided into laminar state or turbulent state. In laminar flow, the fluid mainly performs regular layered movements in the mainstream direction, the flow is relatively stable and no mixing occurs between the fluid layers, and the transmission of momentum and energy mainly depends on the diffusion of molecules; In laminar flow, in addition to the fluid moving in the mainstream direction, there is also a turbulent and random vortex movement of the fluid micelles. At this time, the transmission of momentum and energy occurs not only in the mainstream direction, but also in a direction perpendicular to the mainstream. Therefore, under the same conditions, the heat transfer intensity during fluid turbulence is stronger than that during laminar flow.

(4) Physical properties of fluid

The physical properties of the fluid, such as the density, dynamic viscosity, thermal conductivity, and constant pressure heat capacity, all have an effect on the velocity and temperature distribution of the fluid in the flow field, which will affect the convective heat transfer strength of the fluid.

(5) Geometric factors of heat transfer surface

The surface where the fluid is in contact with the heat exchanger and exchanges heat may be referred to as the heat exchange surface. The size, shape, roughness, and arrangement of the

heat transfer surface will affect the convective heat transfer between the fluid and the heat transfer surface. Therefore, in the case of designing different types of heat exchangers, these factors need specific analysis and research.

As can be seen from the above, there are many factors that affect convective heat transfer, so the methods for improving the heat transfer performance of heat exchangers will vary according to different factors. For different manufacturing and operating conditions, there are different suitable methods to enhance the heat transfer performance of heat exchangers. For PCHE-type compact heat exchangers, the internal heat exchange is mainly through forced convective heat exchange of fluids in microchannels. Therefore, when researching how to optimize such heat exchangers, it is mainly to adopt a technique to increase the convective heat transfer coefficient and reduce the thermal resistance in order to achieve an increase in the heat exchange capacity of the heat exchanger without causing excessive pressure drop in the fluid[36]. According to the influencing factors of convective heat transfer, the way to strengthen the heat transfer process in the heat exchanger can be:

- (1) Increase the total heat transfer area in the heat exchanger
- (2) Increase the average heat transfer temperature difference between cold and hot flow
- (3) Increase the heat transfer coefficient

In general, increasing the total heat transfer area of a heat exchanger to improve heat transfer is a direct and effective method. However, for the traditional shell-and-tube heat exchanger, increasing the total heat transfer area usually results in a greater weight and volume of the heat exchanger, which leads to an increase in manufacturing cost and space occupation. The ideal design solution is to increase the heat transfer area per unit volume of the heat exchanger to increase its compactness while ensuring that the volume of the heat exchanger is unchanged. For

compact heat exchangers similar to PCHE, the heat transfer area per unit volume of the heat exchanger can be increased by increasing the number of channels inside the heat exchanger.

There are two methods used to change the average temperature difference between hot and cold fluids. One is to change the form and configuration of the flow arrangement inside the heat exchanger, such as changing the parallel-flow arrangement to a counter-flow arrangement or a crossflow flow arrangement, or using another suitable flow arrangement design. Under the same operating conditions, the average temperature difference between the hot and cold fluid inside the heat exchanger with different flow arrangement forms and configurations will be different; the other is to change the temperature difference between the hot and cold fluid inlet and outlet. However, in practical applications, limited by factors such as operating conditions and physical properties of the heated material, the selection range of the temperature of the hot and cold fluid at the inlet and outlet of the heat exchanger is usually not very abundant, which restricts the use of the second method.

The heat transfer coefficient in the heat exchanger is related to many factors such as the cause of fluid flow, the phase transition of the fluid, the physical properties of the fluid, and the geometric factors of the heat transfer surface. Theoretically, methods such as increasing the flow velocity of the fluid, destroying the fluid boundary layer, and designing the cylindrical bodies inside the heat exchanger that fluid flows around can improve the convective heat transfer coefficient[37]. For compact heat exchangers similar to PCHE, the heat transfer in the channel can be enhanced by changing the traditional straight channel inside the heat exchanger to a curved S-shaped channel. Its mechanism for enhancing heat exchange is that the curved microchannels will not only extend the flow path of the fluid in the channel but also damage the flow boundary layer and hinder its development, thereby achieving the purpose of enhancing heat transfer [38].

In this study, the methods of increasing the heat transfer area and changing the channel structure will be used mainly to improve the heat transfer of the heat exchanger.

2.1.2 Theoretical Calculation Formula

The two key indicators for measuring the performance of a heat exchanger are the heat transfer performance and pressure drop of the fluid. The heat transfer performance of heat exchangers is usually analyzed using the logarithmic mean temperature difference (LMTD) method or the effective number of transfer unit (ε -NTU) method. The LMTD method is convenient for determining the overall heat transfer coefficient based on the measured inlet and outlet fluid temperatures. The ε -NTU method is convenient for predicting the outlet fluid temperature when the heat transfer coefficient and inlet temperature are known.

The heat exchange rate of heat and cold flow in the heat exchanger can be obtained by the following formula:

$$Q_h = \dot{m}_h C_{p,h} (T_{h,in} - T_{h,out}) \quad (2 - 1)$$

$$Q_c = \dot{m}_c C_{p,c} (T_{c,in} - T_{c,out}) \quad (2 - 2)$$

where the subscripts h and c represent hot and cold fluids, and the subscripts in and out designate the fluid inlet and outlet conditions.

The fluid heat transfer capacity rates are defined as:

$$C_h = \dot{m}_h C_{p,h} \quad (2 - 3)$$

$$C_c = \dot{m}_c C_{p,c} \quad (2 - 4)$$

$$C_{min} = \min(C_h, C_c) \quad (2 - 5)$$

$$C_r = \frac{C_{min}}{C_{max}} \quad (2 - 6)$$

where C_h and C_c are the heat transfer rates of the hot and cold fluids, respectively. C_{min} is the minimum fluid capacity rate, and C_{max} is the maximum fluid capacity rate. C_r is the heat capacity-rate ratio.

The heat transfer performance of the heat exchanger can be measured by analyzing the heat exchanger effectiveness and the overall heat transfer coefficient of the heat exchanger. The effectiveness ε of the heat exchanger is the ratio of the actual heat transfer in the heat exchanger to the maximum heat transfer that can be achieved physically, which is defined as:

$$\varepsilon = \frac{Q_h}{Q_{max}} = \frac{C_h(T_{h,in} - T_{h,out})}{C_{min}(T_{h,in} - T_{c,in})} \quad (2 - 7)$$

The overall heat transfer coefficient of the heat exchanger depends on the conductivity of the heat transfer wall separating the two fluids and the convection coefficient on both sides of the heat transfer wall.

The average heat exchange rate Q_m of the heat exchanger, the overall heat transfer coefficient U and the overall heat exchanger conductance UA value [29] can be obtained by the LMTD method, and they may be computed from the following equation:

$$Q_m = \frac{Q_h + Q_c}{2} \quad (2 - 8)$$

$$U = \frac{Q_m}{A\Delta T_m} \quad (2 - 9)$$

$$UA = \frac{Q_m}{\Delta T_m} \quad (2 - 10)$$

where A is the heat transfer area, ΔT_m is the logarithmic mean temperature difference. The mean temperature difference as defined is the logarithmic mean value as:

$$\Delta T_m = \frac{\Delta T_1 - \Delta T_2}{\ln\left(\frac{\Delta T_1}{\Delta T_2}\right)} \quad (2 - 11)$$

With

$$\Delta T_1 = T_{h,in} - T_{c,out} \quad (2 - 12)$$

And

$$\Delta T_2 = T_{h,out} - T_{c,in} \quad (2 - 13)$$

The heat loss of the heat exchanger is mainly due to the fact that the heat exchanger cannot be completely insulated in actual operation, so that in addition to most of the heat obtained from the heat source is transferred to the cold flow, part of the heat will be transferred to the surrounding.

The heat loss Q_{loss} can be calculated by the following formula:

$$Q_{loss}(\%) = \frac{|Q_h - Q_c|}{Q_h} \quad (2 - 14)$$

In addition to the total heat transfer coefficient U and overall heat exchanger conductance, UA value, the Nusselt number Nu can be used as a parameter to measure the convective heat transfer performance in the channel. The Nusselt number represents the ratio of the conductive resistance to the convective thermal resistance of the working flow in the channel, which is defined as:

$$Nu = \frac{hD_h}{k} \quad (2 - 15)$$

where h is the convective heat transfer coefficient in the channel depending on the fluid properties, flow velocity and channel geometric characteristics, k is the thermal conductivity of the fluid in the channel, and D_h is the hydraulic diameter of the channel. The relationship between the convection heat transfer coefficient h and the total heat transfer coefficient U is:

$$\frac{1}{UA} = \frac{1}{h_h A_h} + \frac{t}{k_s A} + \frac{1}{h_c A_c} \quad (2 - 16)$$

$$A = \min(A_h, A_c) \quad (2 - 17)$$

where t is the solid wall thickness between the hot and cold channels, k_s is the thermal conductivity of the solid material, A_h and A_c are the heat transfer surface area on the hot fluid side and the cold fluid side, respectively. The value of A is usually the maximum value between A_h and A_c .

The hydraulic diameter D_h , the Reynolds number Re , the free flow area A_f and the heat transfer area A on one side of the heat exchanger are calculated by the following relationship:

$$D_h = \frac{4A_{ch}}{P_{ch}} \quad (2 - 18)$$

$$Re = \frac{\rho v D_h}{\mu} = \frac{\dot{m} D_h}{\mu A_f} \quad (2 - 19)$$

$$A_f = N_{ch} A_{ch} \quad (2 - 20)$$

$$A = N_{ch} L P_{ch} \quad (2 - 21)$$

where A_{ch} is the cross-sectional area of each channel, P_{ch} is the cross-sectional perimeter of the flow channel, N_{ch} is the number of channels on one side, and L is the actual length of the channel.

The heat transfer surface area density β is defined as the ratio of the heat transfer area on one side to the volume occupied by the flow channel on this side, which can be calculated by the following formula:

$$\beta = \frac{A_h}{V_h} \text{ or } \frac{A_c}{V_c} \quad (2 - 22)$$

where V_h and V_c are the volumes individually occupied by the hot and cold fluid side heat transfer surfaces.

When measuring the performance of a heat exchanger, in addition to the thermodynamic performance, the pressure drop between the fluid at the inlet and the outlet of the heat exchanger is also worth considering. The pressure drop for the heat exchanger can be obtained from:

$$\Delta p = f \frac{4L}{D_h} \frac{1}{2} \rho v^2 \quad (2 - 23)$$

where f is the Fanning friction factor, which is defined based on the equivalent shear force per unit friction area in the flow direction, and is usually expressed by the relationship with the Reynolds number. It is related to the Reynolds number of the fluid, the surface roughness of the flow channel and the geometric characteristics of the heat exchanger channel. An increase in the Fanning friction factor indicates an increase in the flow resistance of the fluid. Therefore, f can be calculated from:

$$f = \frac{2\tau_s}{\rho v^2} = \frac{P_{in} - P_{out}}{2\rho v^2} \left(\frac{D_h}{L} \right) \quad (2 - 24)$$

where τ_s is the shear stress on the solid wall of the channel, P_{in} is the fluid inlet pressure, P_{out} is the fluid outlet pressure, ρ is the fluid density, and v is the flow velocity.

In addition, Darcy or Moody's friction factor f_D can also be used to represent the flow resistance in the channel, and its calculation relationship with the Fanning friction factor is:

$$f_D = 4f \quad (2 - 25)$$

2.2 Compact Heat Exchangers Design

2.2.1 Flow Arrangement

For the design of compact heat exchangers, the form and configuration of the flow arrangement need to be carefully considered. Different flow arrangement designs will make the temperature distribution inside the heat exchanger different, which will affect the effectiveness of the heat exchanger. At the same time, it has different design and manufacturing difficulties. Therefore, when designing a compact heat exchanger, it is necessary to select a suitable flow arrangement form and configuration according to the desired heat exchanger effectiveness and

manufacturing difficulty. Depending on their form and configuration in the heat exchanger, there are three main types of flow arrangements, and they are:

(1) Counter-flow

In this type of flow arrangement, the two fluids enter the heat exchanger from opposite ends. Each channel in the heat exchanger is parallel to each other.

(2) Parallel-flow

In this type of flow arrangement, the two fluids enter the exchanger at the same end and flow parallel to each other. Each channel in the heat exchanger is also parallel to each other.

(3) Cross-flow

In this type of flow arrangement, the hot and cold fluids typically pass through the heat exchanger perpendicular to each other. The channels of the same fluid are parallel to each other, while the hot and cold channels are roughly perpendicular to each other.

For a single-pass heat exchanger, its heat exchanger effectiveness can be calculated theoretically by the ε -NTU method. The Number of Transfer Units (NTU) for the exchanger is defined as:

$$NTU = \frac{UA}{C_{min}} \quad (2 - 26)$$

After obtaining the value of NTU, combined with the heat capacity-rate ratio obtained by Equation(6), the theoretical value of the heat exchanger effectiveness can be obtained by the ε -NTU method. For a single pass heat exchanger in the parallel-flow arrangement, the effectiveness is expressed as[3]:

$$\varepsilon = \frac{1 - \exp[-NTU(1 + C_r)]}{1 + C_r} \quad (2 - 27)$$

For a single pass heat exchanger in the counter-flow arrangement, the effectiveness is defined as:

$$\varepsilon = \frac{1 - \exp[-NTU(1 + C_r)]}{1 + C_r \exp[-NTU(1 - C_r)]} \quad (2 - 28)$$

Similarly, for a single pass heat exchanger in the cross-flow arrangement, the effectiveness can be defined as:

$$\varepsilon = \frac{1}{C_r} \{1 - \exp[-C_r + C_r \exp(-NTU)]\} \quad (2 - 29)$$

Under the same thermodynamic conditions, the counter-flow arrangement of heat exchanger usually has the highest heat transfer efficiency[39], the reason is that its average temperature difference along any unit length is the highest. In contrast, the parallel-flow arrangement usually has the lowest heat transfer efficiency, while cross-flow arrangement has intermediate thermodynamic performance. The temperature distribution diagram of the heat exchanger under different flow channel arrangements is shown in Figure 1.

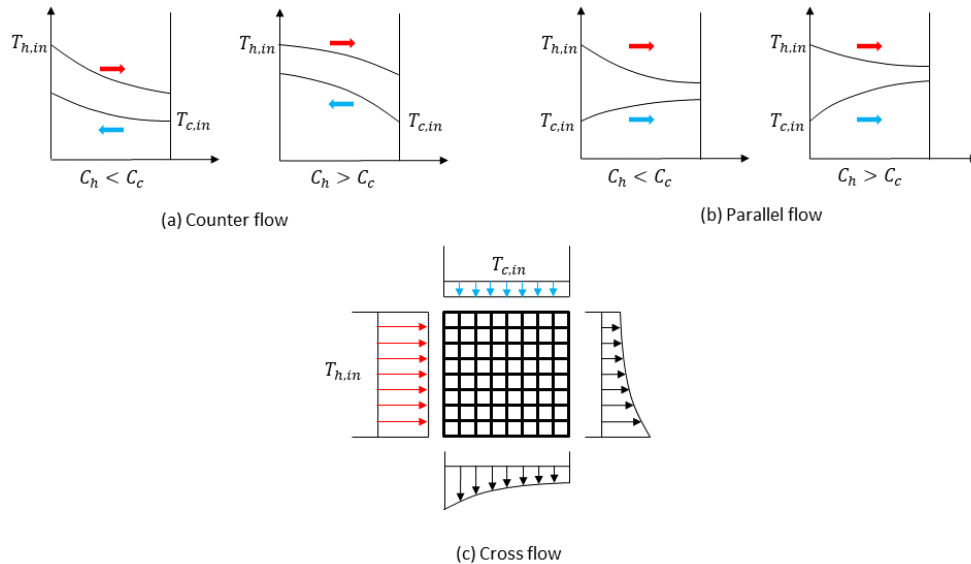


Figure 1 Typical temperature distributions in heat exchangers

However, although the counter-flow arrangement provides the highest heat or cold recovery for the heat exchanger, it must separate the fluid at each end of the heat exchanger and then re-aggregate the same type of fluid. As a result, the geometric design of the header distributor channel is complicated, resulting in design and manufacturing difficulties for compact heat exchangers with counter-flow arrangement[3].

For compact heat exchangers, cross-flow is the most common flow arrangement[3]. While it has high heat exchange performance, there is no need to separate different fluids at the inlet and outlet of the heat exchanger like a counter-flow arrangement, which greatly simplifies the geometric design of the header distributor channel and reduces manufacturing costs.

In addition to the above three main process arrangement methods, the combination any of these flow configurations will also be considered in actual design. For example, cross-counter flow arrangement is a combination of cross-flow and counter-flow arrangement. In this arrangement, one fluid flows in a straight path, while the second fluid follows a zigzag path perpendicular to the first flow. While negotiating the zigzag path, the flow directions of the two fluids in the straight part are parallel and opposite to each other. Therefore, this flow arrangement can be regarded as a global counter-flow, while it remains locally as a cross-flow.

2.2.2 Channel Cross-sectional Shape

When a compact heat exchanger similar to PCHE is manufactured using the DMLS method, the design of the cross-sectional shape of the flow passage is not restricted. Therefore, in addition to manufacturing semi-circular channels according to the standard PCHE, other channel cross-sectional shapes can also be selected to improve the performance of heat exchangers based on the flow and heat transfer characteristics of fluids in the channels of different cross-sectional shapes.

Bahman et al. [3] provide a comparison of some common channel cross-sectional shapes with the same hydraulic diameter when the fluid in the channel is laminar, which is shown in Table 1.

Table 1 Comparison of laminar-flow solutions for different cross-sectional shape

Cross section	Nu	fRe
Triangle	2.35	13.33
Circle	3.66	16.0
Square	2.89	14.2
Rectangle (b/a=4)	4.65	18.3
Rectangle (b/a=8)	5.95	20.5
Rectangle (b/a= ∞)	7.54	24.0

Note that a and b represent the width and length of the rectangle, respectively. The above data applies to the case where $L/4R_h > 100$, where L and R_h represent the length and hydraulic radius of the channel, respectively. It can be seen from the Table 1 that as the cross section of the channel gradually becomes flat, the Nusselt number increases, which means that the convection heat transfer capacity of the channel is enhanced. The main reason is that the rectangular cross-section of aspect ratio (b/a) is flat in shape and usually provides the smaller frontal area, which increases the Reynolds number in the channel at the same flow. As a result, convective heat transfer is enhanced, which is reflected numerically as an increase in Nusselt number. Simultaneously, the friction factor also increases, mainly because the perimeter of the section increases as the shape of the section becomes flatter. When these channels have the same roughness, the longer the perimeter of the channel cross-section, the greater the frictional force experienced by the fluid. In

addition, stress concentration also occurs at the corners of the cross section of the channel, which also results in increased resistance on the fluid. In addition, stress concentration will occur at the corners of the cross section of the channel, which also results in an increase in the friction factor in the channel.

Lee et al. [24] compared the heat transfer performance and friction coefficient of semicircular and circular cross-section channels with the same hydraulic diameter using ANSYS software. The simulation results show that the semicircular cross-section channel is about 4.5% higher in heat transfer effectiveness and 5.3% higher in friction factor than the circular cross-section channel. This shows that under the same number of channels and operating conditions, although the heat transfer characteristics of semicircular channels are better than circular channels, the pressure drop will be larger due to the larger friction factor. Therefore, a trade-off needs to be made between efficiency and coefficient of friction when choosing the shape of the channel cross section.

With the same hydraulic diameter, the ratio of the cross-sectional area of the circular cross-section channel to the semi-circular cross-section channel is as follows:

$$\frac{A_{circle}}{A_{semicircle}} = \frac{2\pi^2}{(2 + \pi)^2} = 0.746 < 1 \quad (2 - 30)$$

For manufacturing compact heat exchangers like PCHE with a fixed volume, the smaller cross-sectional area of the circular cross-section channels means that a larger number of channels with a circular cross-section can be arranged when the cross-section of the heat exchanger is fixed. This makes the overall heat exchange area of the heat exchanger larger, thereby increasing the heat exchange capacity of the heat exchanger. More importantly, the advantage of a smaller friction factor for circular cross-section channel can be utilized to reduce the fluid pressure drop. Therefore,

when manufacturing compact heat exchangers, it may be considered to use a circular cross-section channel instead of a semicircular cross-section channel.

In addition, the use of rectangular cross-section channels with rounded corners can also be considered. When taking advantage of the good heat transfer characteristics of rectangular cross-section channels, the rounded corners can reduce the friction factor to a certain extent. In conclusion, the design of the channel cross-sectional shape of the compact heat exchanger requires a comprehensive consideration.

2.2.3 Wall Thickness between Channels

For the design of compact heat exchangers, after determining the flow arrangement and cross-sectional shape of the heat exchanger channels, the solid wall thickness between each channel needs to be considered.

The thickness of the wall is mainly determined by the maximum design pressure inside the heat exchanger. According to the heat exchanger design part of ASEM[40], the minimum wall thickness calculation formula for circular channels is:

$$t_{min} = \frac{PR}{SE - 0.6P} \quad (2 - 31)$$

where P is the internal design pressure, R is the channel radius, S is the maximum allowable stress value of the material, and E is the joint efficiency.

For standard PCHE, the maximum pressure inside the channel during operation can be up to 500 bars. The joint efficiency E is 1 for seamless channels. Because the compact heat exchanger manufactured by using the DMLS method is integrated, no assembly is required. The material used to manufacture compact heat exchangers can be stainless steel, such as SS316, due to its high

thermal conductivity and good corrosion resistance. In the range of -30 to 100 degrees Celsius, the maximum allowable stress parameter of SS316 is 138MPa according to the part of ASEM about the metric properties of various materials[41].

3.0 Research Description

3.1 Objective

The goal of this study was to investigate the feasibility of applying the DMLS method to construct compact heat exchangers similar to PCHE. Since there is no design limitation of the geometric structure when manufacturing metal objects by the DMLS method, it is possible to get rid of the constraints caused by the original manufacturing method of PCHE, and to consider the employing different channel cross-sectional shape, structure and the interval to improve the performance of the manufactured compact heat exchangers. However, the use of the DMLS method to introduce metal objects introduces a degree of change in surface roughness and geometric characteristics. However, metal objects manufactured by the DMLS method have a certain degree of surface roughness. Therefore, the surface roughness of the channel and its influence on the flow resistance also need to be explored.

3.2 Tasks

The first step of the task was to design and build a PCHE-like compact heat exchanger models based on typical PCHE design data. Then design and build models of three other types of heat exchangers, which have the same volume and the same hydraulic diameter as the first type of heat exchanger, but with different flow channel characteristics. The second step of the task was to manufacture the above-mentioned compact heat exchangers by the DMLS method, build and

assemble an experimental setup for measurement testing. The third step was to measure the heat transfer performance and pressure drop of the four heat exchangers under the same conditions, and then analyze the suitable method for designing the heat exchangers based on DMLS. The fourth step was to measure the surfaces roughness of the channel in the heat exchangers, and discuss the differences of the surface roughness when the build direction and channel cross-sectional shape are different. The last task is to perform measurements of flow pressure losses in different channels.

4.0 Experimental Details

4.1 Compact Heat Exchangers Manufactured by DMLS Method

The heat exchangers in this study were manufactured using direct metal laser sintering (DMLS) 3D printing method. The entire heat exchanger is integrated, while a typical PCHE is formed by stacking multiple metal plates. The DMLS equipment used in this study was the EOSM290 machine housed in the ANSYS Additive Manufacturing Research Laboratory at University of Pittsburgh. Figure 2 shows the photograph of the compact heat exchangers made of stainless SS316 by the DMLS method. These heat exchangers are in the cross-flow arrangement, and the actual size of each heat exchanger is $25.4 \times 70 \times 90$ mm.

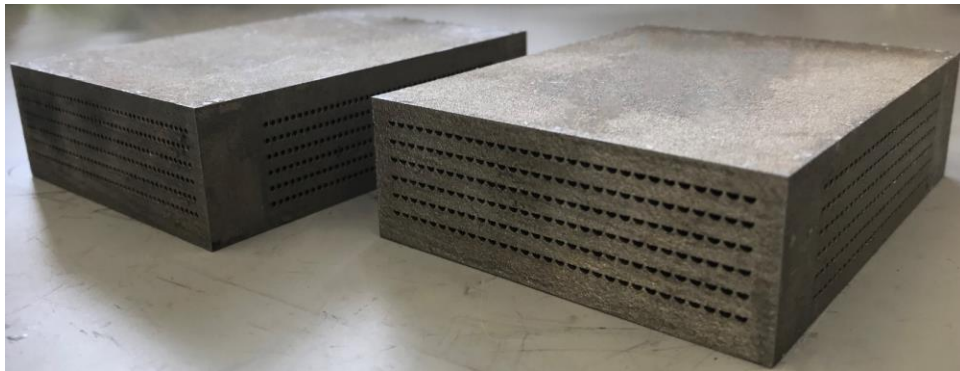


Figure 2 Photograph of the compact heat exchangers

4.1.1 Four Types of Compact Heat Exchanger Designs

In this study, four different stainless compact heat exchangers were manufactured and investigated. The hydraulic diameter of the channels in each heat exchanger is about 1 mm. Figure 3 shows the cross-sectional models and views of four types of compact heat exchangers manufactured. Type 1 is the heat exchanger manufactured according to the structure of a standard cross-flow PCHE heat exchanger. It has a straight channel structure and a semicircular channel cross-sectional shape. The structural parameters of this Type 1 are set according to the typical PCHE. The distance between the two channels in the vertical direction is 1.6mm. The distance in the horizontal direction is the minimum wall thickness between channels at a design pressure of 500 bars.

Type 2 has the cross-sectional shape of the channel changed from semicircular to circular, compared to Type 1. Under the same hydraulic diameter, the area of a circle is smaller than that of a semicircle, thus more channels can be arranged on a fixed cross section of the heat exchanger, which increases the total heat exchange area. In addition, since the circular channel has a smaller friction factor than the semicircular channel[24], the pressure drop of the fluid passing through the heat exchanger can be reduced by taking advantage of this characteristic. Type 2 also has straight channels, and the interval between the channels is the minimum wall thickness calculated according to the heat exchanger design part of ASEM[40]. Therefore, the channels are arranged to the densest on the fixed-size cross section of the heat exchanger.

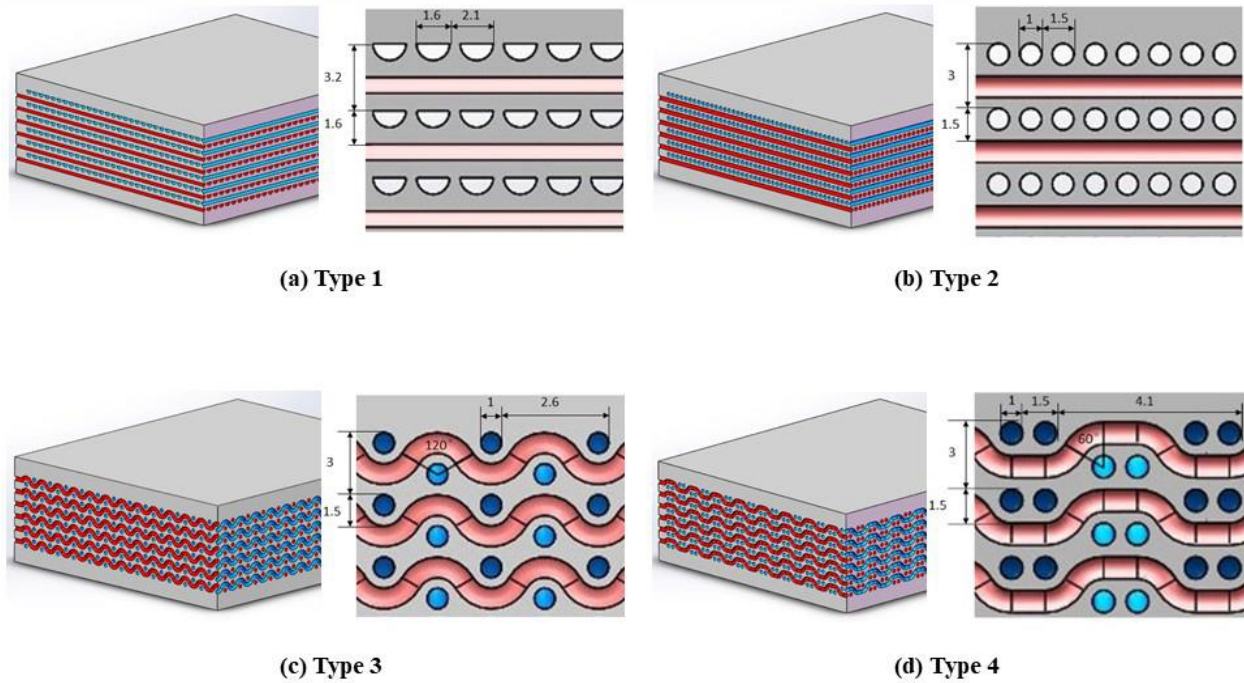


Figure 3 Four different types of compact heat exchangers investigated in this study

For Type 3, the cross-sectional shape of the channel remains circular. The straight channel is changed to an S-shaped curved channel that is curved in the vertical direction, the purpose is to increase the heat transfer coefficient of the channel, because curved microchannels can destroy the flow boundary layer of the fluid and hinder its development. On the other hand, the cold flow channel and the hot flow channel are staggered with each other, which increases the contact area between each cold flow channel and hot flow channel. However, since the curved geometry increases the volume occupied by each channel, the number of channels that can be arranged in a fixed volume is reduced.

Type 4 decreases the bending curvature of the channels on the basis of Type 3 to reduce the volume occupied by each channel, making it possible to arrange more channels under a fixed heat exchanger volume. Type 4 is similar in structure to Type 3, the channels are curved, the cross-

sectional shape of the channels is circular, and the cold flow channels and hot flow channels inside the heat exchanger are also interweaved. The specific design parameters of the four types of heat exchangers are shown in Table 2.

Table 2 Design parameter table of compact heat exchanger

		Type 1	Type 2	Type 3	Type 4	
Channel cross section shape		semicircle	circle	circle	circle	
Geometric diameter of the channel cross section		1.6mm	1mm	1mm	1mm	
Hydraulic diameter of the channel cross section		0.98mm	1mm	1mm	1mm	
Number of channels	Hot side	180	258	150	192	
	Cold side	180	258	150	192	
Channel interval in the horizontal direction		2.1mm	1.5mm	2.6mm	1.5mm	4.1mm
Channel interval in the vertical direction		1.6mm	1.5mm	1.5mm	1.5mm	
Channel length	Hot side	70mm	70mm	83mm	79mm	
	Cold side	90mm	90mm	111mm	101mm	
Angle of the curved part		/		120°	60°	
Radius of the curved part		/		1.5mm	1.5mm	
Dimensions of CHE (H × W × L)		25.4×70×90mm	25.4×70×90mm	25.4×70×90mm	25.4×70×90mm	

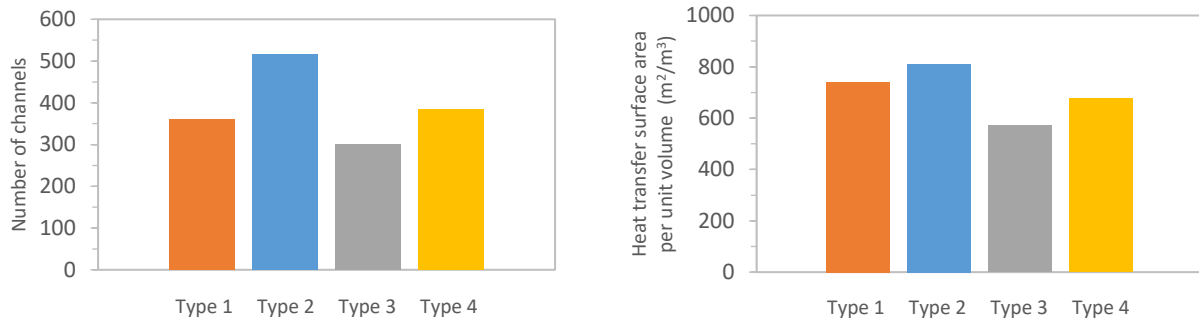


Figure 4 Total number of channels and total heat transfer area of compact heat exchanger

Figure 4 shows the total number of internal channels and heat transfer surface area per unit volume of compact heat exchanger. As can be seen from the figure, Type 2 has the largest number of channels and heat transfer area, while Type 3 has the least, and Type 1 and Type 4 occupy the middle position.

4.1.2 Experiment Setup and Conditions

Figure 5 shows the model of the experimental setup test section. The framework of the test section that house the AM made stainless steel PCHE is made of plexiglass. During the experiment, the heat exchanger is installed in the middle of the test section, and the gaskets are placed on each contact surface between the heat exchanger and the experimental setup. The four chambers formed between the heat exchanger and the experimental device are the inlet and outlet chambers for cold air and hot air, and there are three thermocouples inside each chamber to measure the average temperature of the air. At the same time, two pressure gauges are connected to the test section to record the pressure drop of cold air and hot air through the heat exchanger, respectively.

In actual experiments, air was used as the fluid medium. Two float flowmeters were used to measure the air flow rate on the cold and hot sides. All contact surfaces inside the experimental setup were sealed with grease to ensure no gas leakage. The entire experimental device was covered with sponges to minimize heat loss. Before performing experiments, each measuring device was calibrated. Figure 6 is the actual photograph of the experimental setup.

Figure 7 is the schematic diagram of the experimental setup. The main principle is to use air as the fluid medium of the heat exchanger to test the heat transfer performance and pressure drop of four different types of compact heat exchangers. During the experiment, the inlet hot air temperature was maintained at about 52 degrees Celsius by the heater, and the inlet cold air temperature was about 25 degrees Celsius. The air flow rate used in the experiment was in a range of 6.5 to 37.7 L/min, where the flow and pressure drop were both stable. The temperature data collected by the thermocouple was transmitted to the computer for recording via the acquisition device. Pressure drop data was obtained by recording the value displayed on the pressure gauge within ten minutes under steady state, and the data acquired rate was once every minute.

The experimentally measured parameters include the temperature, pressure, velocity and mass flow of the air flow. The uncertainty in the thermocouples was ± 0.1 K. The uncertainty in the pressure gauges was ± 0.05 Pa. The uncertainty in the float flowmeter was ± 1 SCFH.

Figure 8 shows the temperature record from the beginning of the experiment to the steady state, which tests the performance of Type 1 at an air flow rate of 28.27 L/min. For each experimental test, the criterion for reaching steady state is that the temperature change within ten minutes does not exceed two percent.

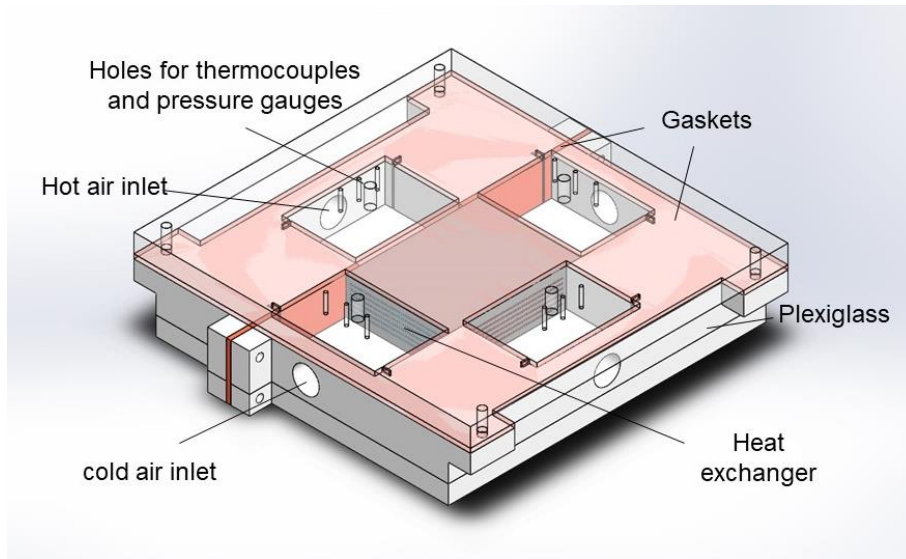


Figure 5 Model of the experimental setup test section



Figure 6 Photograph of the experimental setup

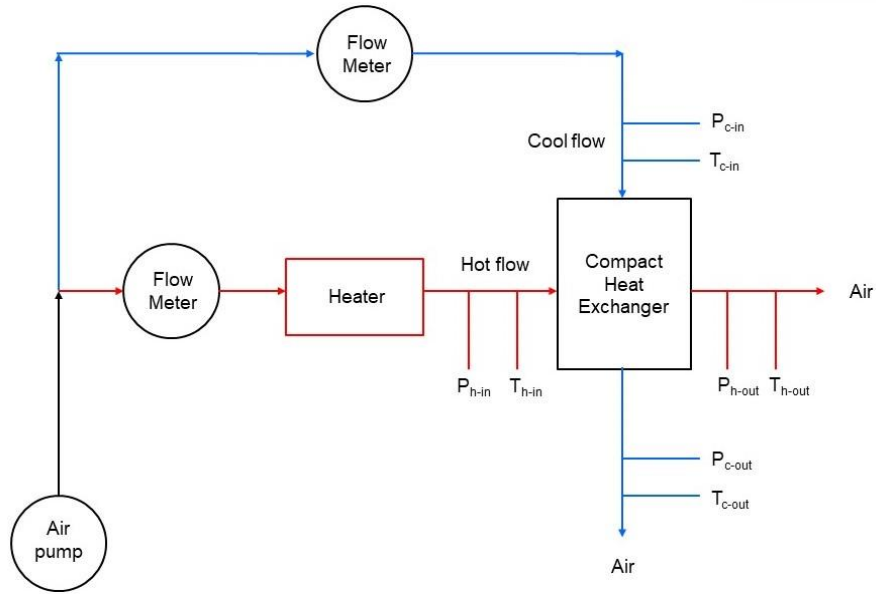


Figure 7 Schematic diagram of the experimental setup

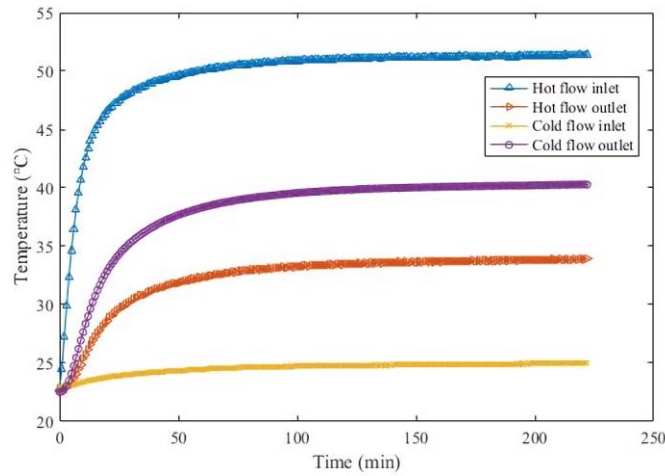


Figure 8 Temperature chart

4.1.3 Experiment Results and Discussion

Figure 9 shows the heat transfer characteristics of the four types of heat exchangers measured for various air flow rate conditions. For each type of heat exchanger test, the flow rate

or Reynolds number of the cold air inlet are kept the same as those of the hot air inlet, and the inlet temperature of hot air and cold air remained at 52 and 25 degrees Celsius, respectively. Figure 9a shows the heat exchanger effectiveness measured keeping the same flow rate on both sides. The heat exchanger effectiveness is higher for Type 2 than Type 1 as the same inlet conditions. However, the heat exchanger effectiveness of Type 3 is the lowest, and the effectiveness of type 4 is slightly lower than that of Type 1. Note that the Type 1 is designed as a standard PCHE.

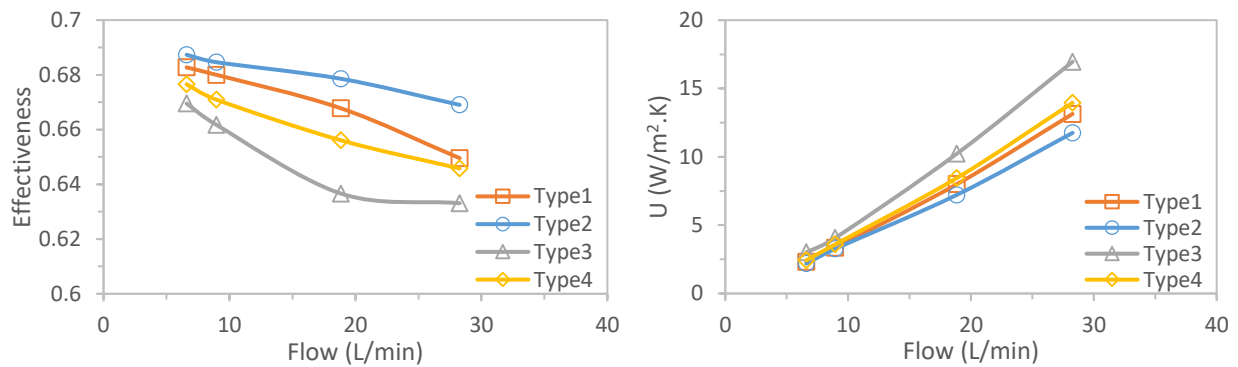


Figure 9 Heat exchanger effectiveness and the overall heat transfer coefficient with the same flow rate

Figure 9b shows the overall heat transfer coefficient measured with the same flow rate maintained on both sides. Type 3 and Type 4 have higher overall heat transfer coefficient than Type 1 and Type 2, and it is obvious that Type 3 has the highest overall heat transfer coefficient, which is of an opposite trend in Figure 9a. It seems that although the curved channel structure of Type 3 and Type 4 improves the heat transfer coefficient compared to the straight channels structure of Type 1 and Type 2, the total number of channels that can be arranged in a fixed volume is reduced, which leads to the total heat transfer area of these two type heat exchangers becomes smaller. As a result, the reduction of the heat transfer area reduces the heat exchanger effectiveness.

Figure 10 shows the average heat exchange rate and overall heat exchanger conductance, defined as UA, of these four types heat exchangers, measured for various Reynolds number conditions on the hot and cold sides. Both of these two parameters are related to the heat transfer performance of the heat exchanger.

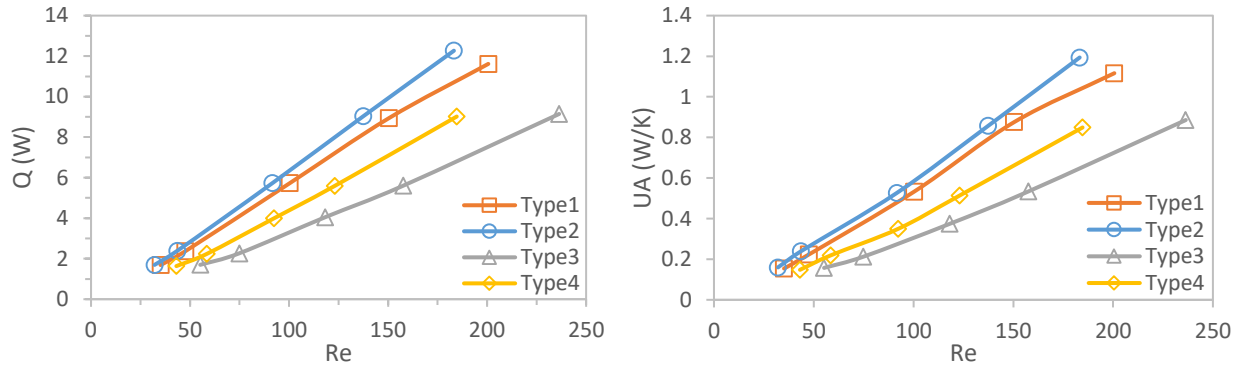


Figure 10 Average heat transfer rate and the overall heat exchanger conductance with the same Reynolds number

As shown in Figure 10, the heat transfer performance of the four types of heat exchangers increases with an increasing Reynolds number. In comparison with other three types of heat exchangers, Type 2 has the largest average heat transfer rate and overall heat exchanger conductance at the same Reynolds number. More importantly, it can be seen from the Figure 10b that the total heat transfer coefficient values in order from small to large are Type 1, Type 2, Type 4, and Type 3. Therefore, the difference between the four heat exchangers' heat transfer performance in Figure 10 can be attributable to the difference in heat transfer area. This can indicate that the heat transfer area plays a more important role in the heat transfer performance for such compact heat exchangers using air as the fluid medium.

Figure 11 shows the average pressure drop of the hot-side and cold-side air according to the change of the air flow rate. The air flow rate at the hot-side inlets is always the same as that at cold-side inlet. As the air flow rate increases, the pressure drop becomes greater due to the increase in flow resistance. Compared with Type 1, Type 2 has a larger number of channels, which increases the free flow area, and as a result, the pressure drop of Type 2 is smaller. The pressure drop and its increasing trend of Type 3 and Type 4 are larger than those of Type 1 and Type 2 due to the reduction in the number of channels and curved channels. With similar curved channel structure, Type 4 has a smaller pressure drop than Type 3 because it increases the number of channels and reduces the bending angle of the channel. Consequently, it can be seen that increasing the number of channels to increase the free flow area can effectively reduce the pressure drop.

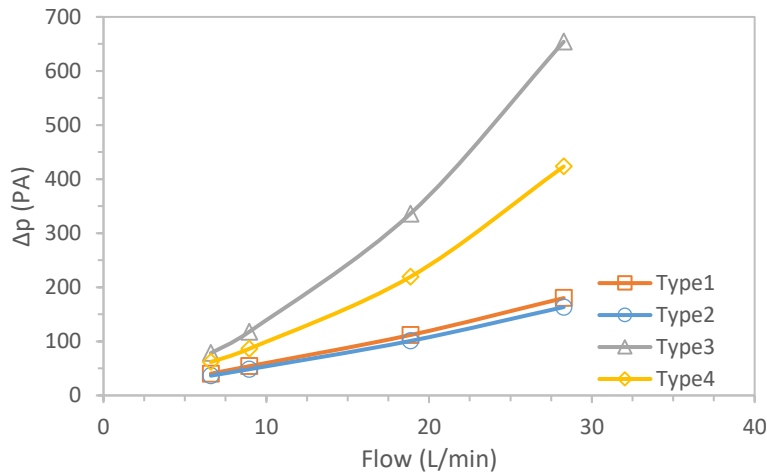


Figure 11 Average pressure drop with the same flow rate on hot and cold sides

Figure 12 shows the average Fanning friction factor of the hot-side and cold-side air according to the change of the Reynolds number, which is calculated using Equation (24). The Reynolds number of the hot-side and cold-side air is the same. The increase of the Reynolds number represents the increase of the flow rate in the channel. As the Reynolds number increases,

the graph shows the tendency of the average Fanning friction factor to decrease. It can be explained from Equation (24) that the Fanning friction factor is inversely proportional to the square of the average flow velocity of the fluid, so the friction factor will decrease as the fluid flow velocity increases.

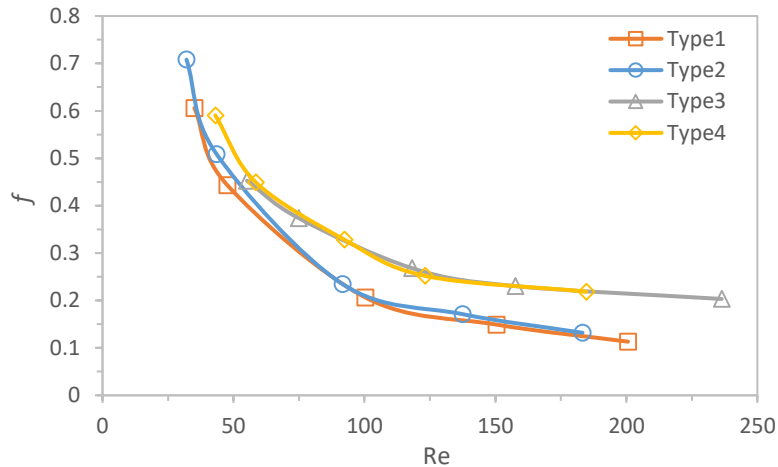


Figure 12 Average Fanning friction factor with the same Reynolds number on hot and cold sides

In addition to the fluid flow velocity, the friction factor is also related to the equivalent shear force of the channel wall. As shown in Figure 12, Since the Type 1 and Type 2 heat exchangers have straight channels inside, which reduces the flow resistance, their fanning friction factors are lower than those of the Type 3 and Type 4 heat exchangers whose channels are S-shaped structures. According to the simulation performed by Lee et al[24], the fanning friction factor of a circular channel is smaller than that of a semicircular channel. However, the average fanning friction factors obtained in this study for Type 1 and Type 2 heat exchangers are nearly the same. One possible reason is that the inner wall surface of the heat exchanger channel manufactured by the DMLS method cannot be perfectly smooth and has a certain degree of roughness. Our experience in operating additive manufacturing machines, also confirmed by other researchers[31],

suggests that surface roughness is related to the shape and size of the cross section of the channel and the build direction. As a result, the surface roughness inside a channel will increase the equivalent shear force, elevating the friction factors. The surface roughness inside the channel will be measured and studied in the next chapter.

In order to comprehensively compare the performance of the four types of heat exchangers, a relative performance coefficient η is introduced, which is defined as:

$$\eta = \frac{\varepsilon/\varepsilon_1}{(\Delta p/\Delta p_1)} \quad (4 - 1)$$

where ε is the heat exchanger effectiveness, Δp is the pressure drop, the subscripts 1 represents the Type 1 heat exchanger, because the Type 1 is used as a contrast.

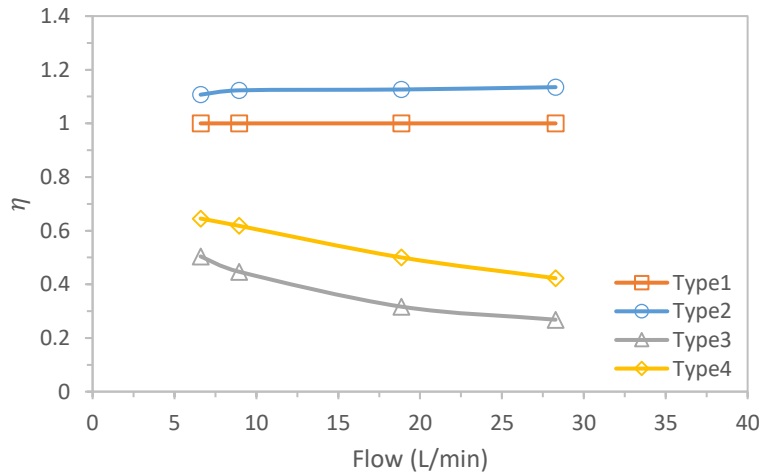


Figure 13 Relative performance coefficient η with the same flow rate

As shown in Figure 13, at the same flow rate, the Type 2 heat exchanger has the best performance, and its coefficient of performance is about 13% higher than that of the Type 1 heat exchangers. Type 3 and Type 4 are significantly lower, the magnitudes of their heat exchanger effectiveness are lower than that of Type 1 and the pressure drops are relatively high, resulting in

lower levels of performance overall. To a certain extent, the lower performances of Type 3 and Type 4 are somewhat unexpected.

In this study, air is used as the fluid medium in the heat exchanger and the air flow rate ranges from 6.5 to 37.7 L/min. The thermal conductivity of air is lower compared to the liquid medium, and due to the low air velocity, the heat transfer coefficient of the heat exchanger is also lower. Therefore, for such compact heat exchangers using air as the fluid medium and operating at low air flow rate, the influence of increasing the heat exchange area of the heat exchanger by directly increasing the number of channels is more important than the influence of improving the heat transfer coefficient of each channel by bending the channels.

In conclusion, when the fluid medium in the heat exchanger is air and the air flow rate range is 6.5 to 37.7 L/min, the increase in heat transfer area will play a more significant role in improving the overall heat transfer performance of the heat exchanger. Consequently, the Type 2 design method, which is the method that maximizes the number of channels inside the heat exchanger to increase the heat exchange area by the densest arrangement, is more suitable for compact heat exchangers based on DMLS. To improve the performance of Type 3 and Type 4 heat exchangers, one plausible approach is to reduce the volume occupied by each channel and by reducing the angle of channel bending, thereby increasing the total number of channels in the heat exchanger.

4.2 Surface Roughness and Geometric Feature of Channels

DMLS is one of the advanced technologies for metal additive manufacturing. This technology makes it possible to manufacture metal parts with complex geometries and enables rapid manufacturing prototypes. However, the main drawbacks that exist when using DMLS method are that the surface roughness and dimensional deviation of the manufactured metal parts are large, which is an inherent result of this method[42]. Figure 14 shows the cross-sectional view of the heat exchangers manufactured through the DMLS method. The two metal parts shown in the figure are a quarter portion of the straight channel heat exchangers investigated in this study, which are made of stainless steel SS316. Since the flow arrangement of the heat exchangers is cross-flow, this results in different build directions for the channels on different sides. Figure 15 shows the inner view of the channel, where the channel surface is not smooth but has a degree of surface roughness.

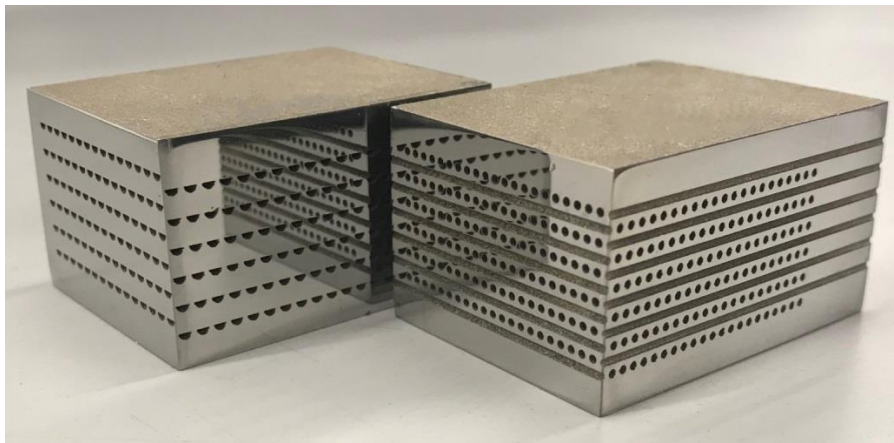


Figure 14 Cross-sectional view of the heat exchangers investigated in this study

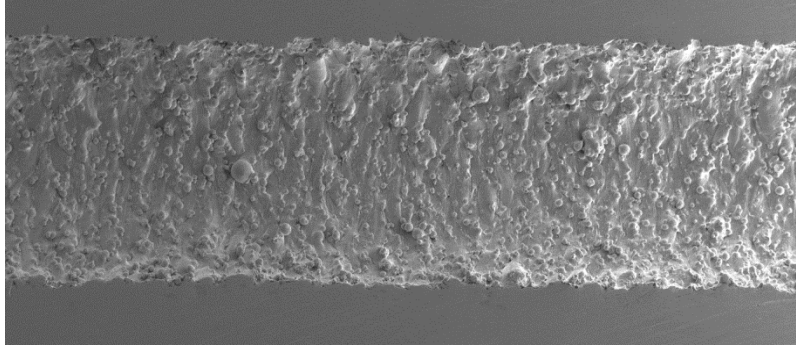


Figure 15 Inner view of the channel through microscope

There is a number of factors that affect the build quality of metal parts manufactured by the DMLS method, such as laser scan speed, scan spacing, material powder, support structure, and build direction[31]. For the heat transfer channels studied here, the build direction, as well as the geometric shape and size of the channel, greatly contribute to the final surface roughness and morphology. Figure 16 shows the morphology differences of four types of channels, the images were obtained by utilizing scanning electron microscope (SEM). The four types of channels were made from the same manufacturing process and materials, but with different geometric shapes and build directions.

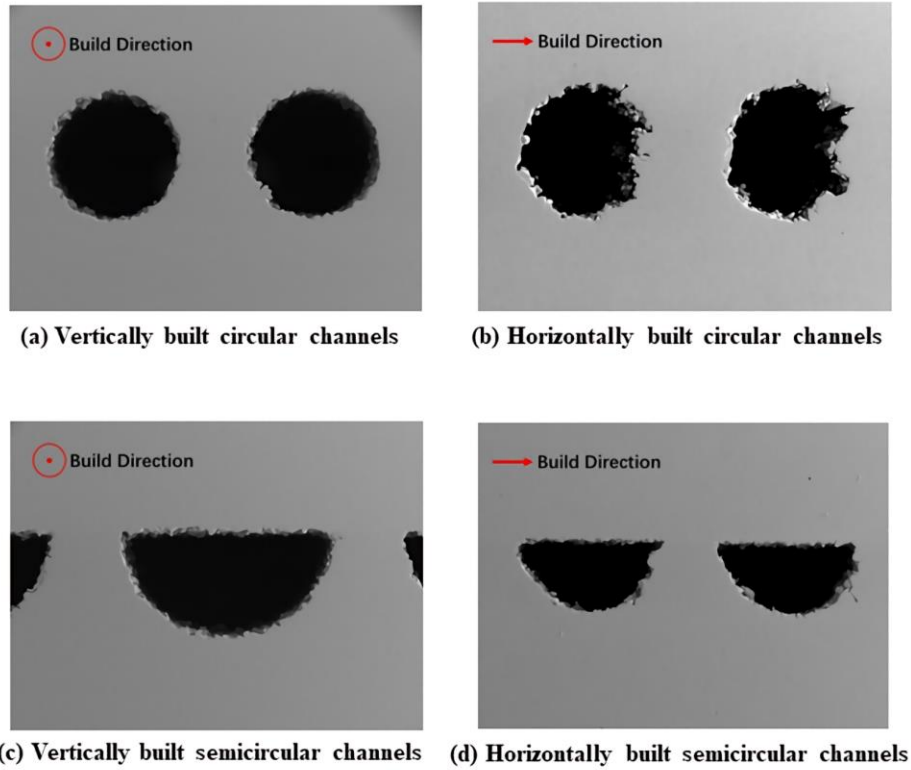


Figure 16 Morphology differences between channels with different build directions and geometric shapes

In Figure 16a, the cross-sectional shape of the channels is circular, and the channels are built vertically, which means that the build direction is parallel to the axial or flow direction of the channel, while in Figure 16b, the cross-sectional shape of the channels is also circular, but the channels are built horizontally, the build direction is perpendicular to the axial direction of the channel. For the channels shown in the Figure 16c and Figure 16d, their cross-sectional shapes are both semicircular, and they are built in the vertical and horizontal directions, respectively. It can be clearly seen that different build directions and geometric shape introduce different characteristics of surface roughness and geometric feature changes. More importantly, since the metal parts are constructed by sintering metal powder layer by layer along the build direction when

using the DMLS method, the surface roughness and shape of the channel edge on the side without the support structure undergoes obvious changes under gravity.

Understandably, roughness and morphological changes in an additive-manufactured channel will affect the pressure loss and heat transfer. Therefore, it is necessary to measure and evaluate the surface roughness and geometric feature in the channels. The purpose of this chapter is to evaluate the average surface roughness and geometric feature changes produced by the DMLS method and their effects on the pressure loss through the heat exchanger channels.

4.2.1 Surface Roughness and Geometric Feature Evaluation

A custom-developed method based on SEM micrographs was adopted for evaluating the surface roughness and geometric features of additive-manufactured channels[43]. Type 1 and Type 2 heat exchangers studied above were cut into four sections in order to capture the surface features of the channels as shown in Figure 17. Therefore, there are a total of six surfaces for each heat exchanger (three surfaces perpendicular to the construction direction and other three surfaces parallel to the construction direction) can be investigated and analyzed by applying SEM images and image segmentation techniques. For each surface, a number of 24 to 50 holes were imaged and analyzed.

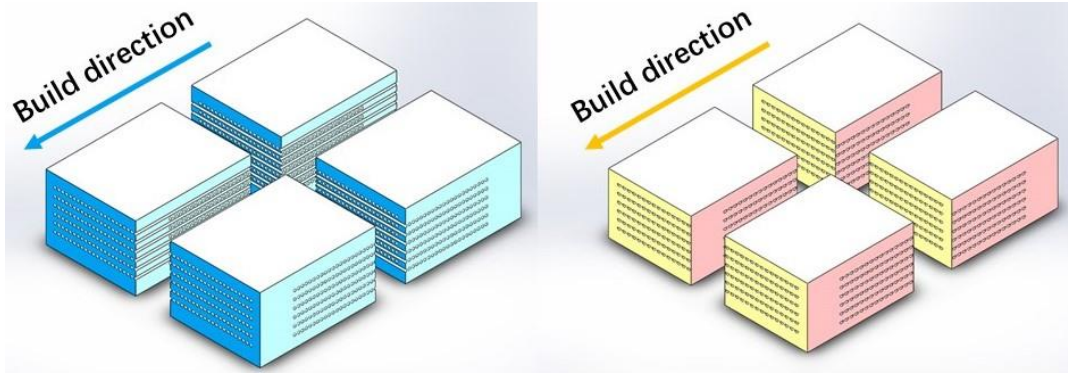


Figure 17 Illustrative graph for heat exchangers cutting

After obtaining the SEM micrographs of each surface, the area occupied by the holes and the geometric profiles of the holes were extracted by judging the grayscales levels, and then the centroid coordinates of each hole can be calculated based on the numerical integration. For a circular hole, the centroid is its center point. For a semicircular hole, the line connecting the center point of the concentric circle and the centroid of the semicircle is perpendicular to its diameter. The distance $\Delta y_{centroid}$ between the center point and centroid of a semicircular hole can be obtained by Equation (4-2):

$$\Delta y_{centroid} = \frac{4R_{semicircle}}{3\pi} \quad (4 - 2)$$

where $R_{semicircle}$ is the designed radius of semicircular channels. The subsequent step is to draw the designed geometric profile of the hole through the positioned center point and the designed radius in a polar coordinate, in which the origin is set at the concentric circle center point of each hole. Figure 18 demonstrates the examples of the designed profiles for different channels. The red crosses in the figure indicate the concentric circle center points of the channel cross-sections.

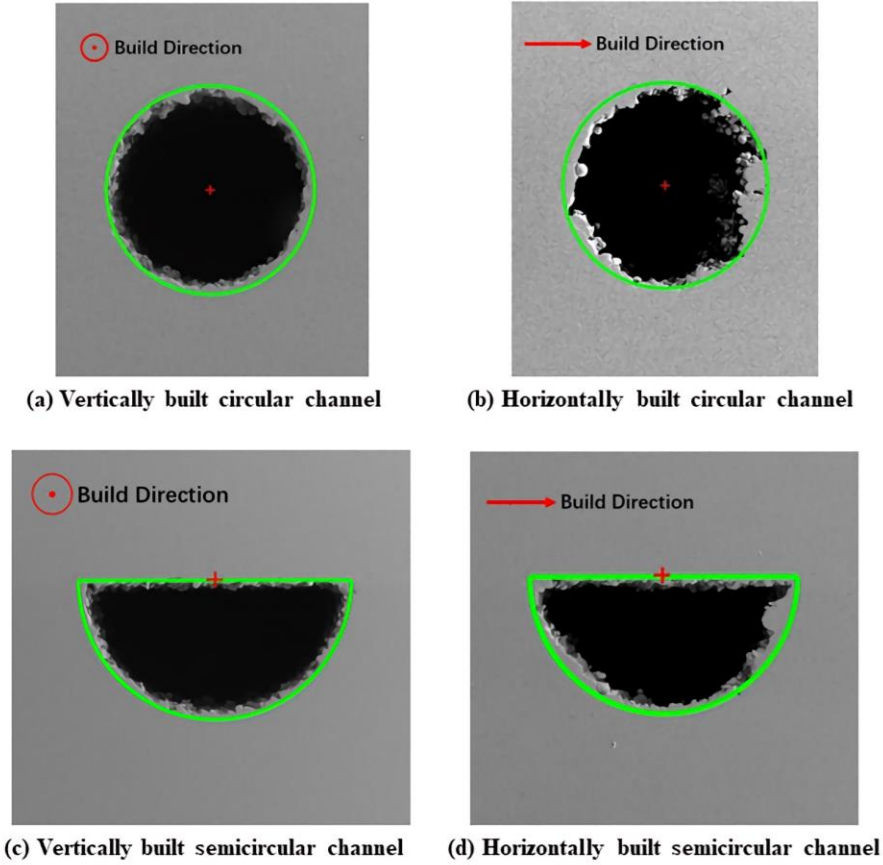


Figure 18 Designed profiles for different channels

The mean radius, R_m , and the arithmetical deviation of the assessed profile for each cut of cross-section, Ra , were evaluated to represent the change in the geometric features of the channels and the average surface roughness, as suggested by Equations (4-3,4). For each type of channel, there were 72 to 150 cross-sectional cuts used to determine the average surface roughness and the actual size of the channels.

$$R_m = \frac{\int R(\theta)d\theta}{2\pi} = \frac{1}{n} \sum_n R_i \quad (4-3)$$

$$Ra = \frac{1}{n} \sum_n |\Delta y_i| \quad (4-4)$$

where R_i is the actual radius of the point selected on the geometric profile, Δy_i is the deviation of the point on the actual profile from the corresponding point on the designed profile.

Figure 19-20 shows the examples of actual profiles for circular and semicircular channels with different build directions. The data line in each figure is the actual profile of the channel cross section, while the nearly centered, horizontal line is the actual average radius. Note that when evaluating a semicircular channel, the cross-sectional profile of the channel is divided into two parts, one is an arc edge part and the other is a straight edge part. The main reason is that the geometric characteristics of the straight edge are different from the arc edge, which leads to different surface roughness. Therefore, the straight part needs to be analyzed separately.

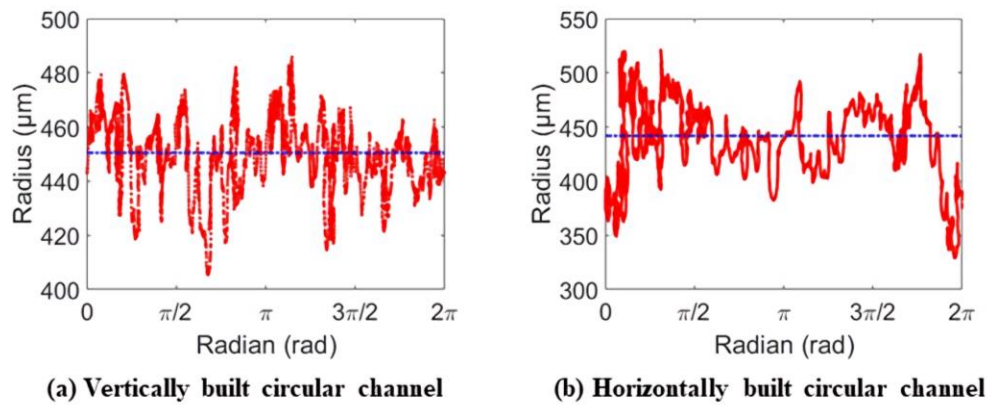
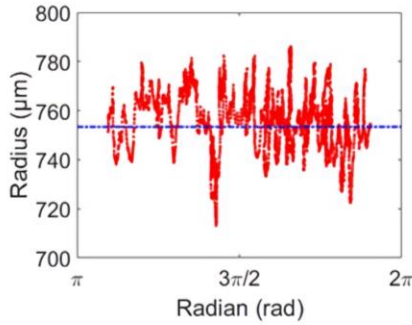
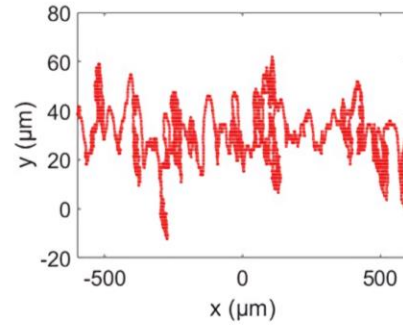


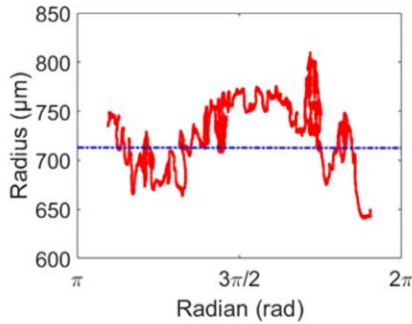
Figure 19 Examples of actual profiles for circular channel



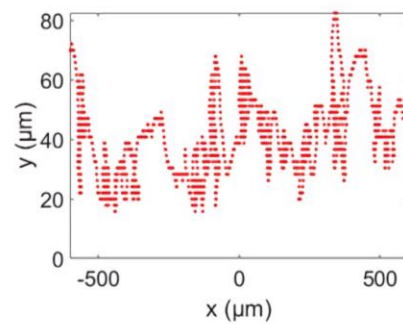
(a) Arc part of vertically built semicircular channel



(b) Straight part of vertically built semicircular channel



(c) Arc part of horizontally built semicircular channel



(d) Straight part of horizontally built semicircular channel

Figure 20 Examples of actual profiles for semicircular channel

Figure 21 demonstrates the comparison of hydraulic radius for different channels, the designed hydraulic radius of each channel is $500 \mu\text{m}$. However, it can be seen that the actual hydraulic radius of the four channels is smaller than the designed hydraulic radius. Compared with semicircular channels, the hydraulic radius of circular channels is smaller on average. Among them, the hydraulic radius of the horizontally built circular channels is the smallest, which is about 17.8% smaller than the designed value. The main reason is that although the circular channels and the semicircular channels have the same design hydraulic radius, the radius of the concentric circle of the semicircular channels is 1.6 times that of the circular channels, which means that the geometric features of the circular channels are smaller. Consequently, when the laser processing diameter is 1mm, channels with smaller geometric features will have greater geometric profile deviations,

which is specifically reflected in the shape, size and surface roughness of the channels. For the channels with the same cross-sectional shape, it is clear that the change in the geometrical features of channels with horizontal build direction is greater than that of channels with vertical build direction. This is because during the DMLS process, the channels are constructed by stacking and sintering metal powder layer by layer. For horizontally printed channels, the metal powder will not immediately condense after being melted by the laser during processing. Due to the lack of a support structure, part of the channel edge will be suspended, causing deformation under the action of gravity. In contrast, for vertically printed channels, this factor has less impact because there are no suspended structures in the design.

Figure 22 demonstrates the comparison of surface roughness for different channels. For channels with the same cross-sectional shape, the build direction has a significant influence on the level of surface roughness. Regardless of the circular channels or the semicircular channels, the surface roughness of the channels introduced through the horizontal build direction is much greater than that introduced through the vertical build direction. The reason is the same as described above. For vertically built channels, the average surface roughness of the circular channels, the arc part and straight part of the semicircular channels is close to each other. The value of the circular channels surface roughness is only about 2% higher than that of other two cases. However, when the build direction is horizontal, the differences among them become more significant. It can be seen that in the horizontal build direction, compared with the circular channels, the straight part of the semicircular channels has the smallest surface roughness, which is about 54.2% lower than that of the circular channels. On the other hand, since the geometric size of the arc part of the semicircular channels is larger than that of the circular channels, this makes the surface roughness of the arc part the semicircular channels slightly smaller than that of the circular channels by about

3%. Therefore, having considered the arc part and the straight part of the semicircular channels, the average surface roughness of the semicircular channels is obviously smaller than the average surface roughness of the circular channels.

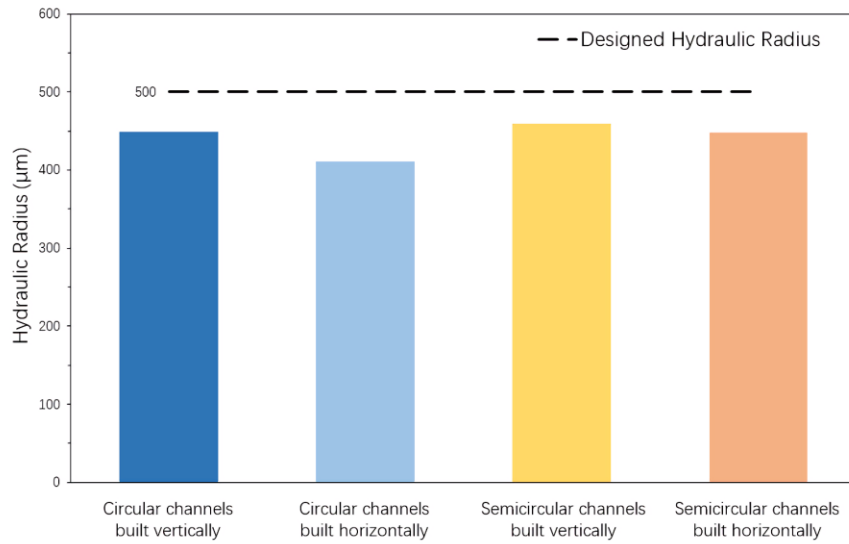


Figure 21 Comparison of hydraulic radius for different channels

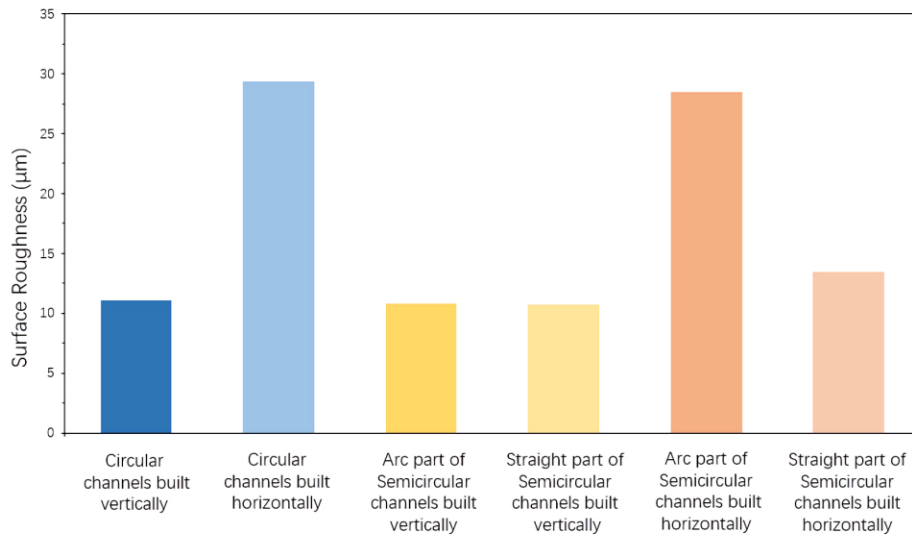


Figure 22 Comparison of surface roughness for different channels

In summary, the build direction has a great influence on the surface roughness and geometric features of the channels. For channels manufactured by the DMLS method, when the designed hydraulic diameter of the channel is 1mm, the surface roughness and geometric feature changes of the semicircular channels are smaller than those of the circular channels. For these circular channels, when the construction direction is changed from vertical to horizontal, the size of the channel will decrease by about 8.4%, the surface roughness will increase by about 165%, and the geometric profile of the cross section will become noticeably irregular. For the semicircular channels with a designed hydraulic diameter of 1mm, when the construction direction is changed from vertical to horizontal, the channel size will decrease by about 2.6%, the surface roughness will increase by approximately 163% in the arc part, and approximately 23.9% in the straight part and the geometry profile of the cross section will also become irregular. Therefore, for the final quality of the manufactured channels, the vertically built semicircular channels have better quality, while the quality of the horizontally built circular channels is worse.

4.2.2 Pressure Drop Characteristics

Before the heat exchangers were cut into four parts, the previous experimental setup was used to measure the pressure drop of these four types of channels. The air inlet temperature is about 25 degrees Celsius and the flow rate ranges from 6.5 to 37.7 L/min. In order to simplify the expression, C1, C2, S1, and S2 will be used in the following figures to represent vertically built circular channels, horizontally built circular channels, vertically built semicircular channels, and horizontally built semicircular channels, respectively. The designed hydraulic diameter of the four

types of channels is 1mm, but due to the processing characteristics of DMLS, the actual hydraulic diameter changes from the designed value.

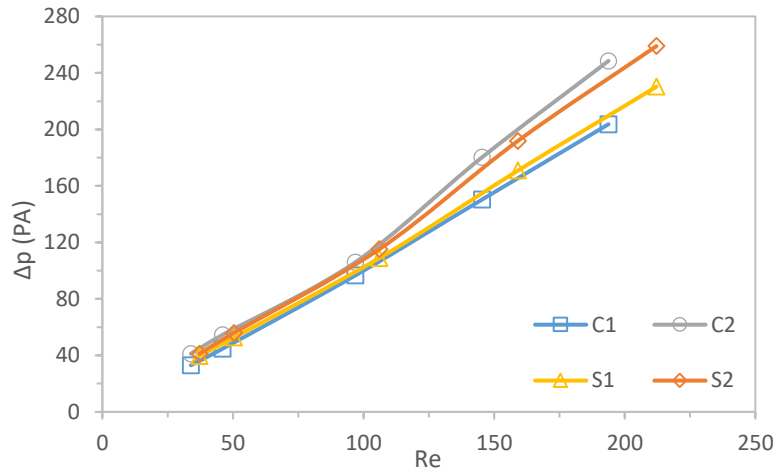


Figure 23 Comparison of pressure drops with the same Reynolds number

Figure 23 demonstrates the pressure drop according the change of Reynolds number. When the Reynolds number is less than 120, the increase in pressure drop for all the four channels is insensitive to Reynolds number. However, when the Reynolds number is greater than 120, the increasing trend of the pressure drop vs. Reynolds number for the channels with the horizontal build direction becomes steeper, due to the changes in surface roughness and geometric features. By applying SEM images and image segmentation techniques, the horizontally built circular channels have the largest average surface roughness and the largest change in geometric features, which results in the highest pressure loss among these channels. In order to further analyze the flow resistance in the channel, consider using the fanning friction factor as a comparison parameter in this study.

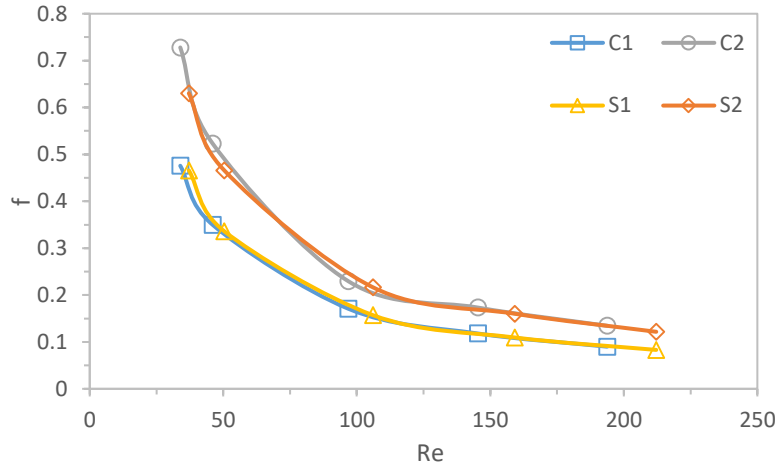


Figure 24 Comparison of the Fanning friction factors with the same Reynolds number

Figure 24 demonstrates the comparison of the fanning friction factors for these four type channels. An increase in the fanning friction factor indicates an increase in the flow resistance of the fluid in the channel. Note that this time the friction factor is calculated by Equation (24) using the actual mean hydraulic diameter of the channel. The fanning friction factor of C1 is slightly lower than that of S1, which indicates that the flow resistance in the circular channel is lower compare to the semicircular channel, even though the surface roughness and geometric feature changes of C1 are slightly higher than those of S1. This means that when the surface roughness and geometric feature changes of the channels manufactured by the DMLS method are similar, the fluid in the circular channel has less pressure loss than that in the semicircular channel.

On the other hand, due to the increase in the surface roughness and geometric feature changes of channels, the fanning friction factor of C2 is 49.6% larger than that of C1, while the fanning friction factor of S2 is 40.9% higher than that of S1. Since the increase of the surface roughness in the straight part of the semicircular channel is not as significant as that in the arc part, which limits the further increase in the flow resistance in the semicircular channel.

In summary, pressure drop testing exhibited that the vertically built channel had a smaller fanning friction factor than the horizontally built channel, which was attributed to differences in surface roughness and geometric feature changes. Therefore, a conclusion can be drawn that the build direction of the channel plays a considerable role in the pressure loss. In addition, for channels manufactured by the DMLS method with the same hydraulic diameter, the vertically built circular channel has the smallest fanning friction factor compared to the other three types of channels. However, when the build direction is horizontal, the increase in fanning friction factor of the circular channel is the greatest, caused by its significant surface roughness and geometric profile distortion.

5.0 Conclusion

In this study, four compact heat exchangers with different channel characteristics were manufactured by the DMLS method of Stainless Steel SS316. This is followed by an experimental study to examine the heat transfer performance and pressure drop of these four types of heat exchangers. The experiment used air as flow medium of laminar regime and the inlet and outlet flow temperatures were kept at 52 and 25 degrees Celsius, respectively. Results from the present study suggest that the heat exchanger of the straight channel with circular cross-sectional shape performs the best, as it inherits high heat transfer performance and low pressure drop, both are attributable to its high total heat transfer surface area and the less restrictive flow cross-section in a fixed volume.

In addition to the thermos-fluid studies on the additive-manufactured compact heat exchangers, SEM images and image segmentation techniques were applied to evaluate the surface roughness and geometric characteristics of circular and semicircular channels with different DMLS build directions. The results show that the vertical build direction leads to better product quality in roughness and geometric features, compared to the horizontal build direction. In addition, the surface roughness and geometric feature changes of the circular channels were generally greater than those of the semicircular channels, due to the smaller geometric features for the circular cross section.

The final task is to study the pressure drop as a result of rough channel caused by different DMLS build directions. If the channel was built in the vertical direction along the channel axis, the flow resistance in the circular channel was slightly smaller than that of the semicircular channel. However, when the build direction was horizontal, this trend is reversed, as the circular cross-

sectional channel presents higher flow resistance, due mainly to the greater changes in the surface roughness and geometric features of the circular channels.

Based on the collective findings of the current study, suggested below are potential follow-up research topics:

- (1) Reduce the bending angle of the curved channel to decrease the volume occupied by each channel, so more channels can be placed in the heat exchanger with a fixed volume, enhancing the overall heat transfer surface area while reducing the pressure drop.
- (2) The cross-sectional shape of the channel can be further optimized with other options, such as a rectangle with rounded corners. The rectangular channel has the potential of elevating heat exchange performance, while the drawback is that its internal friction factor might be high. Adding rounded corners in a rectangular channel eliminates the sharp-edge effect and reduces the flow resistance.
- (3) Explore ways to reduce the surface roughness and geometrical feature changes of heat exchanger channels manufactured by DMLS. This can be accomplished by optimizing the process control and operating parameters, such as laser power, scanning speed, scanning surface spacing and powder selection.

Bibliography

- [1] D. A. Reay, "Compact heat exchangers, enhancement and heat pumps," *Int. J. Refrig.*, vol. 25, no. 4, pp. 460–470, 2002.
- [2] S. S. Mehendafe, A. M. Jacobi, and R. K. Shah, "Fluid flow and heat transfer at micro- and meso-scales with application to heat exchanger design," *Appl. Mech. Rev.*, vol. 53, no. 7, pp. 175–193, 2000.
- [3] D. P. Sekulic, *Compact heat exchangers*. 2018.
- [4] W. xiao Chu, X. hui Li, T. Ma, Y. tung Chen, and Q. wang Wang, "Experimental investigation on SCO₂-water heat transfer characteristics in a printed circuit heat exchanger with straight channels," *Int. J. Heat Mass Transf.*, vol. 113, pp. 184–194, 2017.
- [5] A. M. Aneesh, A. Sharma, A. Srivastava, and P. Chaudhury, "Effects of wavy channel configurations on thermal-hydraulic characteristics of Printed Circuit Heat Exchanger (PCHE)," *Int. J. Heat Mass Transf.*, vol. 118, pp. 304–315, 2018.
- [6] N. Tsuzuki, Y. Kato, and T. Ishiduka, "High performance printed circuit heat exchanger," *Appl. Therm. Eng.*, vol. 27, no. 10, pp. 1702–1707, 2007.
- [7] D. Kwon, L. Jin, W. S. Jung, and S. Jeong, "Experimental investigation of heat transfer coefficient of mini-channel PCHE (printed circuit heat exchanger)," *Cryogenics (Guildf)*, vol. 92, no. March, pp. 41–49, 2018.
- [8] J. H. Jeong, L. S. Kim, J. K. Lee, and M. Y. Ha, "REVIEW OF HEAT EXCHANGER STUDIES FOR HIGH-EFFICIENCY GAS TURBINES," pp. 1–8, 2016.
- [9] K. Thulukkanam, *Heat Exchanger Design Handbook*. 2013.
- [10] C. Desai, H. R. Mehta, and P. Pillay, "Fabrication and Assembly Method for Synchronous Reluctance Machines," *IEEE Transactions on Industry Applications*, vol. 54, no. 5. IEEE, pp. 4227–4235, 2018.
- [11] S. Mylavarapu, X. Sun, J. Figley, N. Needler, and R. Christensen, "Investigation of high-temperature printed circuit heat exchangers for very high temperature reactors," *J. Eng. Gas Turbines Power*, vol. 131, no. 6, 2009.
- [12] D. M. Allen, "Photochemical Machining : from ' manufacturing ' s best kept secret ' to a \$ 6 billion per annum , rapid manufacturing process," no. 2, 1826.
- [13] O. Çakir, A. Yardimedden, and T. Özben, "Chemical machining," vol. 28, no. 8, pp. 499–502, 2007.

- [14] S. K. Mylavarapu, X. Sun, R. N. Christensen, and J. Vaughn, "On the diffusion bonding of Alloy 617 for high-temperature compact heat exchangers," *Transactions*, vol. 101, no. 1, pp. 370–372, 2009.
- [15] S. K. Mylavarapu, X. Sun, R. N. Christensen, R. R. Unocic, R. E. Glosup, and M. W. Patterson, "Fabrication and design aspects of high-temperature compact diffusion bonded heat exchangers," *Nucl. Eng. Des.*, vol. 249, pp. 49–56, 2012.
- [16] A. Simchi, F. Petzoldt, and H. Pohl, "On the development of direct metal laser sintering for rapid tooling," vol. 141, pp. 319–328, 2003.
- [17] J. Kruth, M. Badrossamay, E. Yasa, J. Deckers, L. Thijs, and J. Van Humbeeck, "Part and material properties in selective laser melting of metals."
- [18] E. Chlebus, K. Gruber, B. Ku, J. Kurzac, and T. Kurzynowski, "Materials Science & Engineering A Effect of heat treatment on the microstructure and mechanical properties of Inconel 718 processed by selective laser melting," vol. 639, pp. 647–655, 2015.
- [19] Y. Yang, D. Wang, X. Su, and Y. Chen, "Design and rapid fabrication of non-assembly mechanisms," *2010 Int. Conf. Manuf. Autom.*, vol. 1, pp. 61–63, 2010.
- [20] B. A. Raj, J. T. W. Jappes, M. A. Khan, and V. D. N. C. Brintha, "Studies on heat treatment and electrochemical behaviour of 3D printed DMLS processed nickel - based superalloy," *Appl. Phys. A*, pp. 1–8, 2019.
- [21] M. C. Leu and A. Arbor, "Additive Manufacturing : Current State , Future Potential , Gaps and Needs , and Recommendations," vol. 137, no. February, pp. 1–10, 2015.
- [22] S. Yoon, P. Sabharwall, and E. Kim, "Numerical study on crossflow printed circuit heat exchanger for advanced small modular reactors," *Int. J. Heat Mass Transf.*, vol. 70, pp. 250–263, 2014.
- [23] J. Wang, Y. Sun, M. Lu, J. Wang, and X. Yan, "Study on the Thermal-hydraulic Performance of Sinusoidal Channeled Printed Circuit Heat Exchanger," *Energy Procedia*, vol. 158, pp. 5679–5684, 2019.
- [24] S. M. Lee and K. Y. Kim, "Comparative study on performance of a zigzag printed circuit heat exchanger with various channel shapes and configurations," *Heat Mass Transf. und Stoffuebertragung*, vol. 49, no. 7, pp. 1021–1028, 2013.
- [25] N. S. Berbish, M. Moawed, M. Ammar, and R. I. Afifi, "Heat transfer and friction factor of turbulent flow through a horizontal semi-circular duct," pp. 377–384, 2011.
- [26] H. C. Reynolds, T. B. Swearingen, and D. M. McEligot, "Thermal entry for low Reynolds number turbulent flow," 1969.
- [27] J.-J. Hwang, "Heat transfer-friction characteristic comparison in rectangular ducts with slit and solid ribs mounted on one wall," 1998.

- [28] D. E. Kim, M. H. Kim, J. E. Cha, and S. O. Kim, “Numerical investigation on thermal-hydraulic performance of new printed circuit heat exchanger model,” *Nucl. Eng. Des.*, vol. 238, no. 12, pp. 3269–3276, 2008.
- [29] Y.-D. C. and K.-J. L. Jang-Won Seo, Yoon-Ho Kim, Dongseon Kim, “Heat Transfer and Pressure Drop Characteristics in Straight Microchannel of Printed Circuit Heat Exchangers,” *Entropy*, pp. 3438–3457, 2015.
- [30] I. H. Kim, H. C. No, J. I. Lee, and B. G. Jeon, “Thermal hydraulic performance analysis of the printed circuit heat exchanger using a helium test facility and CFD simulations,” vol. 239, pp. 2399–2408, 2009.
- [31] J. C. Snyder, C. K. Stimpson, K. A. Thole, and D. Mongillo, “Build Direction Effects on Additively Manufactured Channels,” vol. 138, no. May 2016, pp. 1–8, 2019.
- [32] K. L. Kirsch and K. A. Thole, “Heat Transfer and Pressure Loss Measurements in Additively Manufactured Wavy Microchannels,” 2019.
- [33] C. K. Stimpson, J. C. Snyder, K. A. Thole, and D. Mongillo, “Roughness Effects on Flow and Heat Transfer for Additively Manufactured Channels,” vol. 138, no. May 2016, pp. 1–10, 2019.
- [34] X. Zhang, R. Tiwari, A. H. Shooshtari, and M. M. Ohadi, “An additively manufactured metallic manifold-microchannel heat exchanger for high temperature applications,” *Appl. Therm. Eng.*, vol. 143, no. July, pp. 899–908, 2018.
- [35] A. Bejan, *Convection Heat Transfer*. Somerset, UNITED STATES: John Wiley & Sons, Incorporated, 2013.
- [36] P. W. Deshmukh, S. V Prabhu, and R. P. Vedula, “Heat Transfer Enhancement for Laminar Flow in Tubes Using Curved Delta Wing Vortex Generator Inserts,” *Appl. Therm. Eng.*, 2016.
- [37] S. Eiamsa-ard and P. Promvonge, “Numerical study on heat transfer of turbulent channel flow over periodic grooves,” *Int. Commun. Heat Mass Transf.*, vol. 35, no. 7, pp. 844–852, 2008.
- [38] W. Q. Tao, Y. L. He, Q. W. Wang, Z. G. Qu, and F. Q. Song, “A unified analysis on enhancing single phase convective heat transfer with field synergy principle,” *Int. J. Heat Mass Transf.*, vol. 45, no. 24, pp. 4871–4879, 2002.
- [39] R. K. Shah and D. P. Sekulic, “Fundamentals of heat exchanger design.” John Wiley & Sons, Hoboken, NJ, 2003.
- [40] “Division 1 Rules for Construction of Pressure Vessels,” *2010 ASME Boil. Press. Vessel Code*, 2010.
- [41] “Part D Properties (Metric),” *2010 ASME Boil. Press. Vessel CODE*, 2010.

- [42] E. O. Olakanmi, R. F. Cochrane, and K. W. Dalgarno, "Progress in Materials Science A review on selective laser sintering / melting (SLS / SLM) of aluminium alloy powders : Processing , microstructure , and properties," *J. Prog. Mater. Sci.*, vol. 74, pp. 401–477, 2015.
- [43] Min, Z., Wu, Y. J., Yang, K. L., Xu, J., Parbat, S. N., Chyu, M. K., 2020. Dimensional Characterizations Using SEM And Surface Improvement With Electrochemical Polishing Of Additively Manufactured Microchannels. ASME Turbo Expo 2020: Turbomachinery Technical Conference and Exposition, June 22-26, 2020, London, England, Paper Number GT2020-14842 (Accepted)